

Chapter 8

Optimal Selection of the Structural Scheme of Compound Two-Carrier Planetary Gear Trains and Their Parameters



Dimitar P. Karaivanov and Sanjin Troha

8.1 Introduction

8.1.1 Optimization of Planetary Gear Trains

8.1.1.1 General

The optimization of gear trains is a mandatory stage of the process of their design in order to increase their quality and reliability.

Gear trains are complex technical objects and their optimization can be done at different levels [1].

Meshing Optimization

There are quite detailed methods for optimizing the parameters of gear meshing; in some of them attention is paid to the design and in others to the technological factors.

In the design approach for optimization of the qualitative indicators of the meshing as an optimization criterion, the load capacity of the gears by contact stresses and bending stresses is most often used [2–7]. The influence of different geometrical parameters of the gearing is studied. In [8] a program for computer-oriented visual construction of gears is presented. The system allows optimization and creating a 3D model of the gear train in an environment of SolidWorks®.

D. P. Karaivanov (✉)

University of Chemical Technology and Metallurgy, Sofia, Sofia, Bulgaria

S. Troha

Faculty of Engineering, University of Rijeka, Rijeka, Croatia

e-mail: stroha@riteh.hr

In [9] the pitches of the gears are selected so that the gear is “accurate at nominal load,” which improves the contact of the tooth surfaces during operation.

Tooth modification is one of the most commonly used ways to increase the gears’ load capacity [10, 11] or to reduce vibration [12].

In [13] the emphasis is on the procedure for the selection of the design parameters (number of teeth, module, tooth face width) in order to optimize the planetary gear trains.

In [1] a profound study of the influence of the addendum modification of spur involute teeth on the dynamic processes in the gear trains is made, and a methodology for determining the most favorable height addendum modification is proposed. It is found that the internal dynamic load in the addendum-modified gears ($h_a^* > 1$) is lower than in the standard ones, as the lowest values are obtained at the transverse contact ratio $\varepsilon_\alpha = \text{integer}$.

In addition to the load capacity, as an optimization criterion, the efficiency is also used [14]. The optimal values of the profile shift coefficients and the number of teeth of both gears are determined. In [15] a multi-objective optimization by efficiency, transverse contact ratio, pressure angle, relative sliding, and tooth form factor are made, and their influence on the generalized criterion is determined by weight coefficients.

Within the framework of the “X-Gear” Collective Research Project (COOL-CT-2006 030433) financed by the European Commission [16], a methodology for reducing the losses in the gearing with the help of optimizing the tooth geometry has been developed. Attention is paid to the improvement of the parameters of the microgeometry (profile shifting, addendum and tooth flank modifications, etc.) and small corrections of the macrogeometry (number of teeth, module, pressure angle, tooth face width, etc). The study is focused on cylindrical planetary gear trains with helical teeth for the automotive industry and wind turbines.

It should be borne in mind that in cylindrical planetary gear trains with spur gears, the efficiency is high enough to be worth optimizing the tooth geometry in order to reduce losses. This does not prevent the possibility of looking for a way to reduce the peripheral velocity of the gear wheels and the sliding velocity in the meshing. More details on tooth geometry optimizing to reduce meshing loss can be found in [17–19].

In the technological approach, the processing modes are optimized in terms of load capacity (maximum permissible contact and bending stresses).

In [20], the negative effect on load capacity from residual stresses after gear cutting is studied. Their size depends on the degree of wear of the tool and the number of teeth of the gear and the tool (shaper cutter). These stresses are minimized by appropriate selection of the parameters of the tool.

Some authors link the technology of gear manufacturing with the technological cost [21] or labor absorption [22, 23]. In this case, the required load capacity of the gearing is considered as a fulfilled condition for all variants of the technological process. The optimal option is sought by the criterion of minimum technological cost or labor absorption.

Gear Train Elements Optimization

The rim and the disk of a gear have a significant impact on the stresses in the teeth. In [24–26] dependencies are derived geometrically and experimentally to determine the optimal thickness of the gear rim, the further increase of which does not significantly reduce the stress in the critical section of the tooth.

Gear-shafts and shafts. The bending and torsional stiffness shall be selected so as to minimize the unevenness of the load in a meshing [27] or in the parallel meshings of split torque gear trains.

Housing. Deformation of the gearbox housing also affects the load distribution, especially in heavy-duty gearboxes, where reducing deformation by thickening the walls is unacceptably material-intensive. For this reason, it is necessary to optimize the shape of the body [28–30]. Significant attention is also paid to reducing noise emission [31].

Gear train arrangement. Total mass is a common optimization criterion [32, 33]. In most cases, the independent parameters are geometric dimensions. Klein [14] proposes a methodology for minimizing gear volume because it is directly proportional to production costs, as a criterion for determining the size of the gears and selected pitting stress limit.

To minimize the dynamic phenomena in the planetary gear trains, various compensating devices are studied [34, 35]. In non-planetary cylindrical gearboxes, resonant modes are avoided by varying the number of teeth [36].

In [1] a general methodology for optimization analysis of gearboxes with cylindrical and bevel gears is proposed on the basis of a technological-economic criterion, which takes into account the complex influence of the design, technological, and economic factors. Dependencies for determining the components of the technological and economic criterion for the main elements of the gearboxes—shafts, gears, housing, and bearings—in different design and technological variants are derived.

8.1.1.2 Optimization of Planetary Gear Trains Arrangement

The pursuit of finding the optimal solution is quite natural in the process of planetary gear trains (PGTs) design.

Based on the initial data in the design (speed ratio and input torque) can be sought different technical and economic *criteria* (target parameters) for optimization—minimum dimensions, minimum mass, minimum volume, maximum efficiency, minimum production costs, etc. The control *parameters* for optimization can be:

- Number of teeth of the sun gear (mostly).
- Profile shift coefficients.
- Material and processing of gears, etc.

In specific cases, only one of the abovementioned criteria (target parameters) can be decisive for the given arrangement and only through it the optimization may be performed.

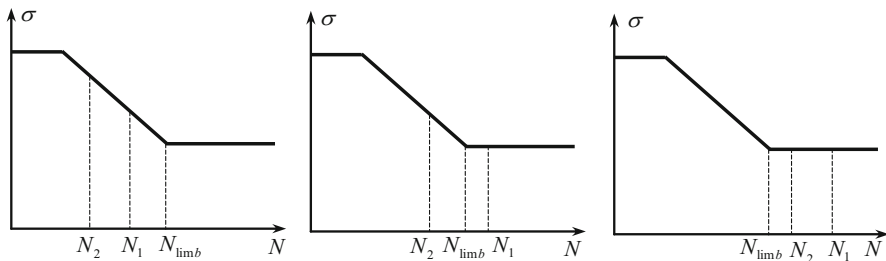


Fig. 8.1 Determination of the stress limit of sun gear 1 and planets 2 at different numbers of load cycles N_1 and N_2

In the general case, however, it is expedient to make optimization according to several criteria—multi-objective (multicriteria) optimization.

When setting the number of teeth in the optimization process, the specific limitations of the type of planetary gear—the conditions for mounting (assembly), coaxiality, and adjacency of the planets—must be taken into account, and keep in mind that these limitations can be avoided [27, 37].

One of the tendencies for PGTs optimizing is to achieve equal strength of the sun gear and planets. In this case, some specific characteristics of PGTs must be taken into account. For the most commonly used $\overline{\text{AI}}$ -PGT (with one external, one internal meshing, and an one-rim planet), these are:

- 1) In non-reversible PGTs, the teeth of the sun gear are loaded in one direction (pulsating loading), and the teeth of the planets are loaded in both directions (completely reversed loading). This fact must be taken into account when determining the bending stress limit (tooth root endurance limit) [27].
- 2) The number of load cycles of the sun gear teeth depends on the number of planets. Figure 8.1 shows the possible cases of the number of cycles N_1 and N_2 of sun gear 1 and planets 2 with respect to base number of cycles N_{limb} (at which long-life fatigue is reached—the knee of Wöhler curve). The number of cycles is determined by formulae known from the literature [27].

The characteristic for $\overline{\text{AI}}$ -PGT placement of all gears (sun gear and planets) inside the ring gear allows the optimization in size (and to a large extent in volume and mass) to be reduced to finding the minimum reference diameter of the ring gear. In this case, the load capacity of the external meshing is authoritative. Some authors accept sufficient to use the contact strength [14, 38], while others consider the bending strength too [23, 39–41].

In [23] a methodology for multi-objective Pareto optimization of $\overline{\text{AI}}$ -PGT by volume, efficiency, mass, and cost is proposed. The respective weight coefficients of the different parameters can be selected for each specific case. A minimum radial overall dimension (ring gear diameter), a maximum efficiency, and minimum clearances (backlash) are the criteria for the multi-objective Pareto optimization of a compound two-carrier PGT proposed in [42]. An arithmetic mean utility function is used.

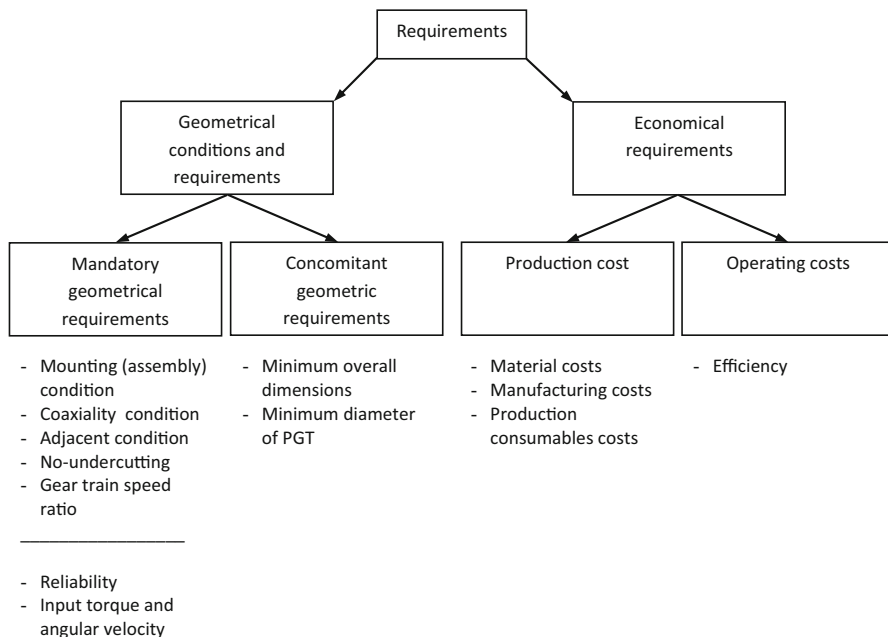


Fig. 8.2 Planetary gear train design requirements (Redrawn from [45])

It should be emphasized that in the multi-objective optimization, the convergence of the different criteria (factors) must be taken into account (Fig. 8.2). Especially at the \overline{AI} -PGT, it can be considered that when achieving a minimum radial dimension (ring gear diameter), minimum (or close to the minimum) mass and volume will be achieved. **At an engineering level, Pareto optimization can be reduced to two criteria—minimum ring gear diameter and maximum efficiency.** Some authors believe that efficiency of \overline{AI} -PGT with spur gears is high enough, and its inclusion in the optimization is only suitable for PGT with helical teeth [43].

It is worth mentioning some other more specialized work on the optimization of PGTs:

In [44] the optimization of the rim thickness of spur ring gear and planets of a simple PGT with high gear ratio is presented. The purpose of optimization is to minimize the total weight for a given power and to determine the minimum thickness of the rim of ring gear and planets. The methodology also allows to find the maximum value of the torque that the train can withstand at a given weight. A new design strategy for design, simulation, and optimization is applied to reduce weight and increase maximum transmitted torque. Tooth geometry is generated using a numerical procedure taking into account the modern manufacturing process. Accurate reproduction of working profiles and fillet curve allows for accurate calculation of contact and bending stresses. Based on a limited number of simulations, many design variants have been generated, and various optimization criteria have been implemented.

Brüser [45] uses multifactor optimization to find the optimal design-technological variant of a two-stage PGT. Fig. 18.3 shows the criteria that the designer must comply with. Of these, four have been selected for optimization purposes—housing diameter, overall dimension, production cost of sun gear, and efficiency. The arithmetic mean utility function is used.

Engineering aspects of PGTs optimization can be found in [27], and more specialized information in [13, 23, 32, 42, 46–51].

8.1.1.3 Optimization as an Element of the Structural Analysis of Planetary Gear Trains

The first step in PGTs design is choosing a structural scheme. Even with this choice, the necessary conditions for obtaining an optimal arrangement must be set. Due to the great variety of PGTs types, in their study it is appropriate to use some structural symbol representing the gear train (regardless of its arrangement) and the external shafts coming out of it. The most convenient is the representation of a simple PGT through the structural symbol of Wolf-Arnaudov. The gear train is represented by a circle, and the three external shafts—with different thickness lines, depending on the size of their torques (this avoids the need to inscribe them, which facilitates the perception of the symbol and reduces the risk of technical errors). Figure 8.3 shows the structural symbol of the most commonly used simple (single-carrier) PGT (AĪ according to [27, 52] or 2 K-H according to Kudryavtsev [27]). In this type of PGT, the torque of the sun gear is the smallest, the torque of the ring gear is greater, and that of the carrier is equal to their sum and is in the opposite direction [27]. This ratio is reflected in the shaft thicknesses on the structural symbol. Other simple (single-carrier) PGTs can also be successfully represented with this structural symbol, but not in all of them the carrier is with the biggest torque [27].

In the *structural analysis* the possibilities for joining several simple (single-carrier) PGTs in a compound (multi-carrier) one are investigated, and in the *optimization* the most suitable combination and its parameters are sought.

In Fig. 8.4 the possible ways of forming a compound two-carrier PGT are shown. In Fig. 8.4a the compound PGT has two single (external) shafts and two compound (one external and one internal) shafts.

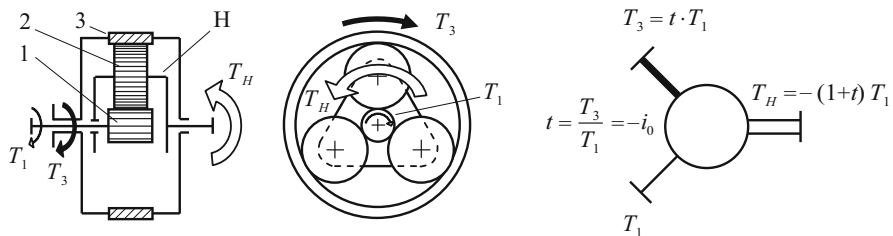


Fig. 8.3 The most common type of simple single-carrier PGT, torques at its central elements, and Wolf-Arnaudov’s symbol (1, sun gear; 2, planets; 3, ring gear; H, carrier)

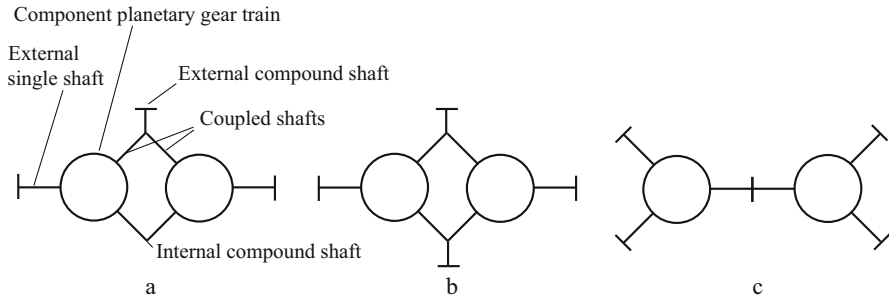


Fig. 8.4 Types of compound two-carrier PGTs: (a) With three external (two single and one compound) shafts. (b) With four external (two single and two compound) shafts. (c) With four external (single) and one internal (compound) shafts

Table 8.1 Possible ways of connecting the two component single-carrier PGTs in a compound two-carrier PGT according to Fig. 8.4a (with three external shafts)

	...1	...2	...3	...4	...5	...6
1...	11	12	13	14	15	16
2...	21 = 12	22	23	24	25	26
3...	31 = 13	32 = 23	33	34	35	36
4...	41 = 14	42 = 24	43 = 34	44	45	46
5...	51 = 15	52 = 25	53 = 35	54 = 45	55	56
6...	61 = 16	62 = 26	63 = 36	64 = 46	65 = 56	66

In the compound PGT in Fig. 8.4b all four shafts (two single and two compound) are external. The PGT in Fig. 8.4c is with four external (single) shafts and one internal (compound) shaft.

Each of the coupled shafts can be with one of the three torques (and for the \overline{AI} -PGT from Fig. 8.3 each of them can be a sun gear, a ring gear, or a carrier). In the first case (Fig. 8.4a) 36 combinations are possible (Table 8.1), 21 of which are

Table 8.2 Possible ways of connecting the two component single-carrier PGTs in a compound two-carrier PGT according to Fig. 8.4b (with four external shafts—two single and two compound)

	...1	...2	...3	...4	...5	...6
1...	11 ≡ 22	12	13 ≡ 24	14 ≡ 23	15 ≡ 26	16 ≡ 25
2...	21 ≡ 12	22 ≡ 11	23 ≡ 14	24 ≡ 13	25 ≡ 16	26 ≡ 15
3...	31 ≡ 13	32 ≡ 23	33 ≡ 44	34	35 ≡ 46	36 ≡ 45
4...	41 ≡ 14	42 ≡ 24	43 ≡ 34	44 ≡ 33	45 ≡ 36	46 ≡ 35
5...	51 ≡ 15	52 ≡ 25	53 ≡ 35	54 ≡ 45	55 ≡ 66	56
6...	61 ≡ 16	62 ≡ 26	63 ≡ 36	64 ≡ 46	65 ≡ 56	66 ≡ 55

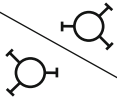
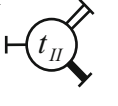
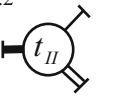
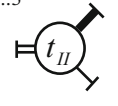
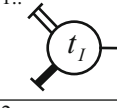
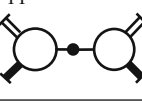
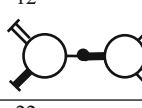
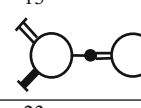
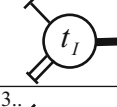
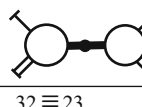
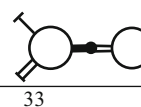
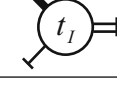
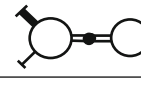
different (non-repeating) [27, 53, 54]. In the second case (Fig. 8.4b) of the 36 combinations (Table 8.2) only 12 are different (non-repeating) [27, 49, 53], and in the third case (Figure 8.4c) the different (non-repeating) schemes are only 6 [27, 53] (Table 8.3).

The main design parameter of the \overline{AI} -PGT (Fig. 8.3) is the ratio of the number of teeth of ring gear z_3 to the number of teeth of sun gear z_1 , on which ratio depends the basic speed ratio of the gear train with a fixed carrier i_0 . The basic efficiency also largely depends on this number of teeth [55–57] as well as the PGT overall dimensions (respectively, volume, mass, material consumption, and labor costs).

Generally speaking, the purpose of optimization can be to choose the structural scheme and its parameters (basic speed ratios of the component PGTs) in which the desired speed ratio is achieved with the best combination of several criteria (e.g., minimum dimensions, maximum efficiency, etc.). After this choice it is possible to proceed to optimization of the arrangement according to other parameters (e.g., the ones listed in Sect. 8.1.1.1).

There are many more combinations for three- and four-carrier PGTs, but the approach discussed in this chapter can be applied to them as well.

Table 8.3 Possible ways of connecting the two component single-carrier PGTs in a compound two-carrier PGT according to Figure 8.4c (with four single external shafts)

	..1 	..2 	..3 
1.. 	11 	12 	13 
2.. 	21 ≡ 12	22 	23 
3.. 	31 ≡ 13	32 ≡ 23	33 

8.1.2 Torque Method: An Easy Way for Planetary Gear Train Analysis

The optimization approaches proposed in this chapter are based on the torque method [27, 58]. This simple and practical method allows easy and very clear determination of the speed ratio and the efficiency. It is very appropriate for investigation of complex compound PGTs [59] as well as for optimization procedures.

The torques on the three external shafts of \overline{AI} -PGT are depicted in Fig. 8.3. They are in a strictly defined ratio, no matter what the operating mode of the gear trains is—with 1 degree of freedom (as a reducer or a multiplier) or with 2 degrees of freedom (as a division or a summation differential).

When the losses are disregarded, i.e., efficiency $\eta_0 = \eta_{13(H)} = \eta_{31(H)} = 1$, this ratio is as follows:

$$T_1 : T_3 : T_H = T_{D\min} : T_{D\max} : T_\Sigma = T_1 : t \cdot T_1 : -(1 + t)T_1 = +1 : +t : -(1 + t) \tag{8.1}$$

where:

- $T_1 \equiv T_{D\min}$ is the ideal torque on the sun gear.
- $T_3 \equiv T_{D\max}$ is the ideal torque on the ring gear.
- $T_H \equiv T_\Sigma$ is the ideal torque on the carrier.

$$t = \frac{T_3}{T_1} = \frac{T_{D \max}}{T_{D \min}} = \left| \frac{z_3}{z_1} \right| > +1 \quad (8.2)$$

is the *torque ratio* of the gear train

$\eta_0 = \eta_{13(H)} = \eta_{31(H)}$ is the basic efficiency of the PGT (with fixed carrier).

These three ideal torques are in equilibrium

$$T_1 + T_3 + T_H = T_{D \min} + T_{D \max} + T_\Sigma = 0. \quad (8.3)$$

Knowing the ideal torques on the shafts and considering which of them is input (with torque T_A and angular velocity ω_A) and output (with torque T_B and angular velocity ω_B) from the equilibrium of the ideal input and output powers

$$P_A + P_B = T_A \cdot \omega_A + T_B \cdot \omega_B = 0, \quad (8.4)$$

the gear train speed ratio (kinematic ratio) is obtained as follows:

$$i_k = \frac{\omega_A}{\omega_B} = -\frac{T_B}{T_A}. \quad (8.5)$$

When the losses are considered, i.e., the basic efficiency $\eta_0 = \eta_{13(H)} = \eta_{31(H)} < 1$, the real torques $T'_1 \equiv T'_{D \min}$, $T'_3 \equiv T'_{D \max}$, and $T'_H \equiv T'_\Sigma$ can be determined as a function of torque ratio t and basic efficiency η_0 of the PGT [27]. From the equilibrium of the real input and output powers

$$\Sigma P = P_A \cdot \eta + P_B = \eta \cdot T'_A \cdot \omega_A + T'_B \cdot \omega_B = 0 \quad (8.6)$$

the efficiency can be obtained:

$$\eta = -\frac{P_B}{P_A} = -\frac{T'_B \cdot \omega_B}{T'_A \cdot \omega_A} = -\frac{\frac{T'_B}{T'_A}}{\frac{\omega_A}{\omega_B}} = -\frac{i_T}{i_k}, \quad (8.7)$$

where:

$$i_T = \frac{T'_B}{T'_A} \quad (8.8)$$

is the so-called *torque transformation (torque transmit ratio)*.

Considering formula (8.5) at last the efficiency can be obtained by torques

$$\eta = -\frac{i_T}{i_k} = \frac{\frac{T'_B}{T'_A}}{\frac{T_B}{T_A}}. \quad (8.9)$$

Formulae (8.5) and (8.9) are very useful for optimization analysis of PGTs.

8.2 Optimal Selection of the Structural Scheme of Compound Two-Carrier Planetary Gear Trains with Three External Shafts

8.2.1 Possible Structural Schemes

Each simple PGT (with the exception of some specific types, such as uncoaxial (open) ones [27]) has three external shafts and is conveniently represented by the Wolf-Arnaudov structural symbol (Fig. 8.3). As mentioned in Sect. 8.1.1.3, depending on the way the three outer shafts of the two assembling gears are connected, 36 combinations are possible, 21 of which are non-repeating (Table 8.1.). From the various features and possibilities provided by the structural Schemes [27], for the purposes of optimization, the following will be considered here:

1. As well as the simple PGT, the compound one has three external shafts with different torques, two of which (the smaller $T_{D\min}$ and the bigger $T_{D\max}$) are unidirectional, and the torque of the third shaft T_{Σ} is opposite, equal to the sum of the other two torques $|T_{\Sigma}| = T_{D\min} + T_{D\max}$.
2. Between the torques on the three external shafts, there are the same dependencies as in the simple PGT

$$\Sigma T_i = T_{D\min} + T_{D\max} + T_{\Sigma} = 0 \text{ and } T_{D\min} < T_{D\max} < |T_{\Sigma}| \quad (8.10)$$

regardless of how the PGT works:

- With one ($F = 1$) or two ($F = 2$) degrees of freedom.
- Which is the fixed element at $F = 1$.
- What is the direction of power flow, i.e., whether the gear train operates as a reducer or multiplier at $F = 1$ or as a summation or division differential at $F = 2$.

3) Similar to simple PGT, it is convenient to define a torque ratio (the ratio of unidirectional torques $T_{D\min}$ and $T_{D\max}$), which can be called an *aligned (reduced) torque ratio* and which depends on the torque ratios t_I and t_{II} of the component PGTs

$$t_{red} = \frac{T_{D\max}}{T_{D\min}} = f(t_I, t_{II}) > 1. \quad (8.11)$$

It has been found that with this torque ratio, the speed ratios of the compound PGT for the six cases of operation with one degree of freedom ($F = 1$) are determined by the same formulae as in the simple PGT [27, 54].

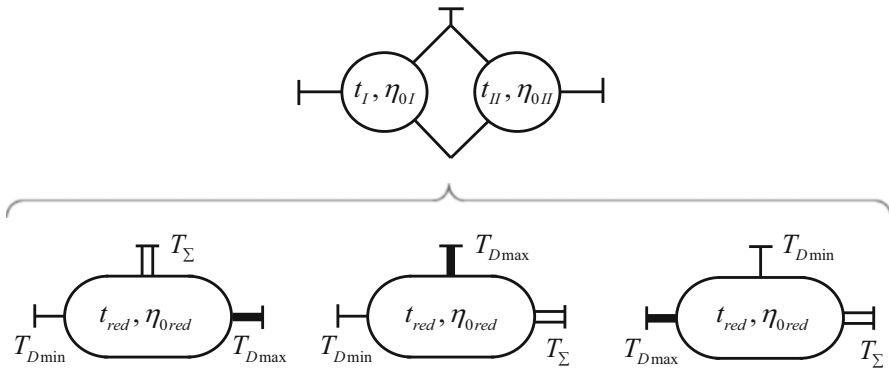


Fig. 8.5 Torques on the external shafts of compound PGTs from Table 8.1

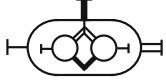
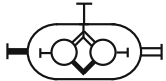

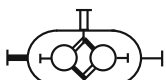
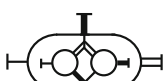
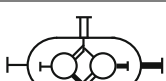
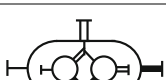
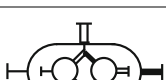
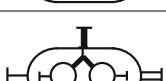
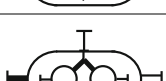
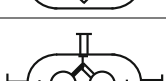
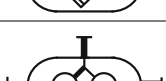
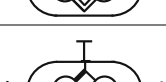
It follows from the above that when deriving formulae for $t_{red} = f(t_I, t_{II})$, for each of the structural schemes from Table 8.1, its kinematic capabilities (lower and upper limit of t_{red}) can be determined at given limits of t_I and t_{II} [54]. It should be borne in mind that in some of the structural schemes, depending on the size of the two torque ratios t_I and t_{II} , a different shaft has the least torque (T_{Dmin}), i.e., the shafts change their role in the gear, but the summation shaft (with T_{Σ}) remains the same (Fig. 8.5).

These formulae are shown in Table 8.4. Representing the dependencies in graphical form allows the designer to quickly find out which of the schemes is worth considering. Figure 8.6 shows, as an example, some of the most interesting cases.

A more detailed approach is also possible, in which the structural schemes for the six cases of operation of each PGT with $F = 1$ degree of freedom should be drawn. For the schemes from Table 8.1, it is convenient to use the designation of the input-output-(fixed) shafts with their position (according to the directions of the world) W-west (left), E-east (right), and N-north (top). For example, WE(N) means the left shaft, input; the right shaft, output; and the top shaft, fixed. These diagrams are shown in Appendix 8.1. For some schemes from the main diagonal of Table 8.1 (S11, S12, etc.) at $t_I = t_{II}$, an infinity for t_{red} is obtained ($t_{red} = \infty$ due to zero in the denominator). In this case the output shaft is immovable, and PGT is idling, i.e., the efficiency is equal to zero.

The first step of any optimization is to select the structural schemes that may provide the required speed ratio, i.e., they should have the appropriate t_{red} , and to apply the optimization procedure to them. By varying t_I and t_{II} , the plurality of combinations thereof are obtained in which the PGT can achieve the desired aligned torque ratio t_{red} . Optimization procedures are applied to this set, and the most appropriate combination of one or more criteria is sought.

Table 8.4 Determination of the aligned torque ratio t_{red} of structural schemes from Table 8.1 as a function of the torque ratios of the component PGTs t_I and t_{II}

Scheme	t_I and t_{II}	Structural symbol	$t_{red} = f(t_I, t_{II})$
S11	$t_I \geq 2 t_{II}$		$\frac{t_I - t_{II}}{t_{II}}$
	$t_{II} \leq t_I \leq 2 t_{II}$		$\frac{t_{II}}{t_I - t_{II}}$
S12	$t_I \geq 1 + t_{II}$		$\frac{t_I}{1 + t_{II}}$
	$t_I \leq 1 + t_{II}$		$\frac{1 + t_{II}}{t_I}$
S13	For every t_I and t_{II}		$t_I \cdot t_{II} - 1$
S14	For every t_I and t_{II}		$\frac{t_I \cdot t_{II}}{1 + t_{II}}$
S15	For every t_I and t_{II}		$t_I + \frac{t_I}{t_{II}}$
S16	For every t_I and t_{II}		$t_I(1 + t_{II})$
S22	$t_I \geq 1 + 2 t_{II}$		$\frac{t_I - t_{II}}{1 + t_{II}}$
	$t_{II} \leq t_I \leq 1 + 2 t_{II}$		$\frac{1 + t_{II}}{t_I - t_{II}}$
S23	For every t_I and t_{II}		$(1 + t_I) t_{II}$
S24	$t_I \geq \frac{2 + t_{II}}{t_{II}}$		$\frac{t_I \cdot t_{II} - 1}{1 + t_{II}}$
	$t_I \leq \frac{2 + t_{II}}{t_{II}}$		$\frac{1 + t_{II}}{t_I \cdot t_{II} - 1}$

(continued)

Table 8.4 (continued)

Scheme	t_I and t_{II}	Structural symbol	$t_{red} = f(t_I, t_{II})$
S25	For every t_I and t_{II}		$\frac{1 + t_I + t_I \cdot t_{II}}{t_{II}}$
S26	For every t_I and t_{II}		$t_I + t_{II} + t_I \cdot t_{II}$
S33	$t_I \geq 2 t_{II}$		$\frac{t_I - t_{II}}{t_{II}}$
	$t_{II} \leq t_I \leq 2 t_{II}$		$\frac{t_{II}}{t_I - t_{II}}$
S34	For every t_I and t_{II}		$t_I + \frac{t_I}{t_{II}}$
S35	For every t_I and t_{II}		$\frac{t_I \cdot t_{II}}{1 + t_{II}}$
S36	$t_I \geq 1 + t_{II}$		$\frac{t_I}{1 + t_{II}}$
	$t_I \leq 1 + t_{II}$		$\frac{1 + t_{II}}{t_I}$
S44	$t_I \geq t_{II}$		$\frac{t_{II} + t_I \cdot t_{II}}{t_I - t_{II}}$
S45	$t_I \geq \frac{1+t_{II}}{t_{II}-1}$		$\frac{t_I \cdot t_{II}}{1 + t_I + t_{II}}$
	$t_I \leq \frac{1+t_{II}}{t_{II}-1}$		$\frac{1 + t_I + t_{II}}{t_I \cdot t_{II}}$
S46	For every t_I and t_{II}		$\frac{1 + t_{II} + t_I \cdot t_{II}}{t_I}$
S55	$t_I \geq t_{II}$		$\frac{t_{II} + t_I \cdot t_{II}}{t_I - t_{II}}$

(continued)

Table 8.4 (continued)

Scheme	t_I and t_{II}	Structural symbol	$t_{red} = f(t_I, t_{II})$
S56	$t_I \geq \frac{2}{t_{II}-1}$		$\frac{t_I \cdot t_{II} - 1}{1 + t_I}$
	$t_I \leq \frac{2}{t_{II}-1}$		$\frac{1 + t_I}{t_I \cdot t_{II} - 1}$
S66	$t_I \geq 1 + 2 t_{II}$		$\frac{t_I - t_{II}}{1 + t_{II}}$
	$t_{II} \leq t_I \leq 1 + 2 t_{II}$		$\frac{1 + t_{II}}{t_I - t_{II}}$

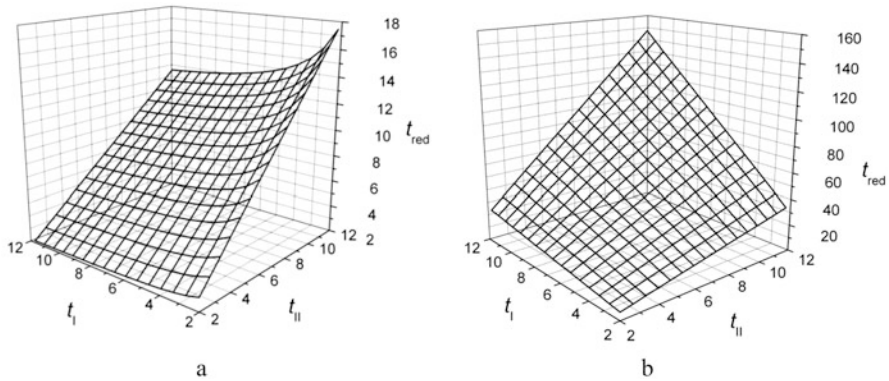


Fig. 8.6 Dependencies of t_{red} as a function of the torque ratios of the component PGTs t_I and t_{II} for several structural schemes from Tables 8.1 and 8.4: a, Scheme 15; b, Scheme 16

8.2.2 Optimization Criteria

8.2.2.1 Overall Dimensions

Compactness, one of the main advantages of PGTs, stems from both the power sharing between the planets and the fact that all the gears are located in the ring gear [27]. For this reason, for optimization purposes, it is very convenient to use the reference diameter of the ring gear as an optimization criterion for the overall PGT size.

From the load capacity of the external meshing (which is the weak point of the gear train), the smallest allowable diameter of sun gear d_1 can be determined. Practice shows that surface durability (pitting) is relevant in this case. At a torque

ratio $t = \frac{z_2}{z_1} > 3$, $z_2 > z_1$ is obtained. In this more common case, according to ISO 6336 [60] the diameter of sun gear 1 is determined as follows:

$$d_1 = \sqrt[3]{Z_H^2 \cdot Z_E^2 \cdot Z_\varepsilon^2 \cdot Z_\beta^2 \frac{2T_1}{k \left(\frac{b_H}{d_1}\right) \sigma_{HP}^2} \cdot \frac{u_{12} + 1}{u_{12}} K_A \cdot K_V \cdot K_{H\beta} \cdot K_{H\alpha} \cdot K_\gamma}, \quad (8.12)$$

where:

Z_H is the zone factor, which accounts for the influence on Hertzian pressure of tooth flank curvature at the pitch point and transforms the tangential load at the reference cylinder to normal load at the pitch cylinder.

Z_E is the elasticity factor, considering the influence of material properties—modulus of elasticity E and Poisson's ratio ν , $\sqrt{\frac{N}{\text{mm}^2}}$.

Z_ε is the contact ratio factor, considering the influence of sum length of contact line (virtual face width) because of double meshing, i.e., the influence of transverse contact ratio ε_α ($\varepsilon_\beta = 0!$)

T_1 is the torque on the sun gear 1.

k is the number of planets.

$\psi_{d1} = \frac{b_H}{d_1}$ is the face width ratio.

$u_{12} = \frac{z_2}{z_1}$ if $z_2 > z_1$, i.e., $t > 3$ (if $z_2 < z_1$, i.e., $t < 3$, the ratio $u_{21} = \frac{z_1}{z_2}$ must be used) is the teeth ratio of the external meshing.

K_A is the application factor, adjusting the nominal load F_t in order to compensate for incremental gear train loads from external sources.

K_V is the internal dynamic factor, accounting for the effects of gear tooth accuracy grade as related to speed and load. Considering meshing variable stiffness as parametric excitation too.

$K_{H\beta}$ is the face load factor, taking into account the effects of the non-uniform distribution of load over the gear face on the surface stress due to inaccuracies, deformations, and bearing clearances.

$K_{H\alpha}$ is the transverse load factor, considering the effect of the non-uniform distribution of transverse load between several pairs of simultaneous contacting gear teeth due to inaccuracies in the base pitch p_b (as well as deflection under load, profile modifications, etc.)

K_γ is the mesh load factor, considering uneven load distribution between planets due to the gears and carrier inaccuracies.

The permissible contact stress is determined as follows:

$$\sigma_{HP} = \frac{\sigma_{H \lim b} \cdot Z_{NT}}{S_{H \min}} Z_L \cdot Z_R \cdot Z_V \cdot Z_W \cdot Z_X, \quad (8.13)$$

where:

$\sigma_{H \lim b}$ is the allowable stress number—contact (pitting endurance limit).

$S_{H \min}$ is the minimum required safety factor (pitting).

Z_{NT} is the life factor for test gears for contact stress.

Z_L is the lubricant factor, which accounts for the influence of the lubricant viscosity.

Z_R is the roughness factor, which accounts for the surface roughness.

Z_v is the velocity factor, which accounts for the influence of pitch line velocity.

Z_W is the work hardening factor, which accounts for the effect of meshing with a surface hardened or similarly hard mating gear.

Z_X is the size factor, which accounts for the influence of the tooth dimensions for the permissible contact stress.

If $t = \frac{z_2}{z_1} < 3$, the case of $z_2 < z_1$ is obtained. In this case by formula (8.12), the reference diameter of planets d_2 is determined. And teeth ratio $u_{21} = \frac{z_1}{z_2}$ must be used. Despite the fact that this case is less common, it is good to take it into account in the calculations and optimization software.

Given that

$$\frac{u_{12} + 1}{u_{12} - 1} = \frac{\frac{t-1}{2} + 1}{\frac{t-1}{2} - 1} = \frac{t + 1}{t - 1}, \quad (8.14)$$

formula (8.12) can be represented as follows:

$$d_1 = K_0 \sqrt[3]{T_1 \frac{t + 1}{t - 1}}, \quad (8.15)$$

where the coefficient K_0 combines the parameters of formulae (8.12) and (8.13) independent of the structural scheme

$$K_0 = \sqrt[3]{Z_H^2 \cdot Z_E^2 \cdot Z_\varepsilon^2 \cdot Z_\beta^2 \frac{2}{k \left(\frac{b_w}{d_1}\right) \sigma_{HP}^2} K_A \cdot K_v \cdot K_{H\alpha} \cdot K_{H\beta} \cdot K_\gamma}. \quad (8.16)$$

In order to obtain comparable results, the same coefficient K_0 must be used in the analysis of all structural schemes. For example, it can be determined under the following conditions (admissions):

1. Cylindrical spur gears with involute profile without shifting are used, i.e., $Z_H = 2.5$ and $Z_\beta = 1$.
2. The gears are made absolutely accurate (without a difference between the errors in the pitch on the base circle f_{pb} , i.e., $\Delta f_{pb} = 0$); this means $K_{H\beta} = 1$.
3. The number of planets is $k = 3$ and the load is evenly distributed between them; this means $K_\gamma = 1$.
4. The influence of the external and internal dynamic load is neglected; this means $K_A = K_v = 1$.

5. The material of gears is a through hardened (tempering) wrought steel with pitting endurance limit $\sigma_{H \text{ lim } b} = 500 \text{ MPa}$ and modulus of elasticity $E = 2.1 \cdot 10^5 \text{ MPa}$; this means $Z_E = 190 \sqrt{\text{MPa}}$.
6. In all gear trains $b_H/d_1 = 0.7$, $Z_N = Z_L = Z_R = Z_V = Z_W = Z_X = 1$, and $K_{H\beta} \cdot Z_e = 1$.

After substitution in formulae (8.13) and (8.16), the following is obtained:

$$K_0 \approx 8, \sqrt[3]{\frac{1}{\text{MPa}}}.$$

Of course, the sun gear diameter can also be determined by the tooth bending strength [60]. It is important that it depends on the torque T_I and the torque ratio t of the PGT. From the kinematics of the gear train and from formulae (8.2) and (8.15) for the reference diameter of ring gear, the following is obtained:

$$d_3 = \frac{z_3}{z_1} d_1 = t \cdot d_1 = K_0 \cdot t \sqrt[3]{T_I \frac{t+1}{t-1}}. \quad (8.17)$$

The reference diameter of ring gear determined in this way can serve as a criterion for the size of the simple PGT depending on its torque ratio t (respectively basic speed ratio i_0).

In the analysis of a compound PGT, the torque on each of the sun gears of the component simple PGTs must be determined as a function of the known torque (usually this is the smallest external torque T_{min} which is an input torque for the gearbox). Using the torque method, it is not difficult to do this for the corresponding structural Scheme [54]. In order to derive these formulae, it is first good to know the relationship between the torques on the sun gears of the two component PGTs. One of these torques is the smallest torque T_{min} in the gear train in general. Table 8.5 shows the formulae for the structural schemes of the compound two-carrier PGTs with two compound and three external shafts from Table 8.1.

In Table 8.6 are defined the torques T_{II} and T_{III} on sun gears of the component PGTs as a function of the smallest external torque $T_{D \text{ min}}$ that is usually an input torque T_A when the gear train operates as a reducer.

With the help of these formulae, by varying the values of the torque ratios of the component PGTs, their influence on the dimensions of the component PGTs, and hence on the size of the compound PGT, can be determined.

8.2.2.2 Efficiency

The high efficiency of PGTs in their operation with a movable carrier is due to the fact that not all transmitted power generates losses, but only that which flows with respect to the carrier. This effect is observed only in PGTs with a negative basic speed ratio $i_0 < 0$. It can be assumed that part of the input (absolute transmitted)

Table 8.5 Determination of the torques T_{I} and T_{II} on the sun gears of component PGTs as a function of the minimal torque T_{\min} in the compound PGT and the torque ratios t_I and t_{II} of the component PGTs

11, 15, 55	12, 14	13, 16, 56
$t_I > t_{II}$ $t_I < t_{II}$ $T_{I} = T_{\min}$ $T_{I} = \frac{t_{II}}{t_I} T_{\min}$ $T_{II} = \frac{t_I}{t_{II}} T_{\min}$ $T_{II} = T_{\min}$	$t_I > 1 + t_{II}$ $t_I < 1 + t_{II}$ $T_{I} = T_{\min}$ $T_{I} = \frac{1+t_{II}}{t_I} T_{\min}$ $T_{II} = \frac{t_I}{1+t_{II}} T_{\min}$ $T_{II} = T_{\min}$	$T_{I} = T_{\min}$ $T_{I} = t_I \cdot T_{\min}$
22, 24, 44	23, 26, 46	12, 45
$t_I > t_{II}$ $t_I < t_{II}$ $T_{I} = T_{\min}$ $T_{I} = \frac{1+t_{II}}{1+t_I} T_{\min}$ $T_{II} = \frac{1+t_I}{1+t_{II}} T_{\min}$ $T_{II} = T_{\min}$	$T_{I} = T_{\min}$ $T_{I} = (1+t_I) \cdot T_{\min}$	$t_I > t_{II} - 1$ $t_I < t_{II} - 1$ $T_{I} = T_{\min}$ $T_{I} = \frac{t_{II}}{1+t_I} T_{\min}$ $T_{II} = \frac{1+t_I}{t_{II}} T_{\min}$ $T_{II} = T_{\min}$
33, 36, 66	34	35
$T_{I} = T_{\min}$ $T_{II} = T_{\min}$	$T_{I} = (1+t_{II}) T_{\min}$ $T_{II} = T_{\min}$	$T_{I} = t_{II} \cdot T_{\min}$ $T_{II} = T_{\min}$

power P_A is transmitted by the entire train (as a coupling) with the movement of the carrier—the so-called coupling power P_{coup} — and the rest is transmitted by the movement of the elements with respect to the carrier, the so-called relative (rolling) power P_{rel} (Fig. 8.7) [27].

The smaller part of input power is the relative (rolling) power; the greater is the efficiency. For the correct determination of the efficiency, it is necessary to know the direction of the relative (rolling) power that can be:

- From the sun gear 1 to the ring gear 3.
- From the ring gear 3 to the sun gear 1.

This depends on which of both elements is input (driving) and which output (driven) for the relative power. Given that the direction of the torque and the angular velocity coincides on the input element and is different on the output element, the following condition can be written with respect to the torque of the sun gear T_I and its relative angular velocity $\omega_{1rel} = \omega_1 - \omega_H$ with respect to the carrier H:

Table 8.6 Determination of the torques T_{1I} and T_{1II} on the sun gears of component PGTs as a function of the minimal external torque $T_{D\min}$ of the compound PGT

Scheme	t_I and t_{II}	Structural symbol	T_{1I} and $T_{1II} = f(t_I, t_{II}, T_{D\min})$
S11	$t_I \geq 2t_{II}$		$T_{1I} = T_{D\min}; T_{1II} = \frac{t_I}{t_{II}} T_{D\min}$
	$t_{II} \leq t_I \leq 2t_{II}$		$T_{1I} = \frac{t_{II}}{t_I - t_{II}} T_{D\min}; T_{1II} = \frac{t_I}{t_I - t_{II}} T_{D\min}$
S12	$t_I \geq 1 + t_{II}$		$T_{1I} = T_{D\min}; T_{1II} = \frac{t_I}{1 + t_{II}} T_{D\min}$
	$t_I \leq 1 + t_{II}$		$T_{1I} = \frac{1 + t_{II}}{t_I} T_{D\max}; T_{1II} = T_{D\min}$
S13	For every t_I and t_{II}		$T_{1I} = T_{D\min}; T_{1II} = t_I \cdot T_{D\min}$
S14	For every t_I and t_{II}		$T_{1I} = T_{D\min}; T_{1II} = \frac{t_I}{1 + t_{II}} T_{D\min}$
S15	For every t_I and t_{II}		$T_{1I} = T_{D\min}; T_{1II} = \frac{t_I}{t_{II}} T_{D\min}$
S16	For every t_I and t_{II}		$T_{1I} = T_{D\min}; T_{1II} = t_I \cdot T_{D\min}$
S22	$t_I \geq 1 + 2t_{II}$		$T_{1I} = T_{D\min}; T_{1II} = \frac{1 + t_I}{1 + t_{II}} T_{D\min}$
	$t_{II} \leq t_I \leq 1 + 2t_{II}$		$T_{1I} = \frac{1 + t_{II}}{t_I - t_{II}} T_{D\min}; T_{1II} = \frac{1 + t_I}{t_I - t_{II}} T_{D\min}$
S23	For every t_I and t_{II}		$T_{1I} = T_{D\min}; T_{1II} = (1 + t_I) T_{D\min}$
S24	$t_I \geq \frac{2 + t_{II}}{t_{II}}$		$T_{1I} = T_{D\min}; T_{1II} = \frac{1 + t_I}{1 + t_{II}} T_{D\min}$
	$t_I \leq \frac{2 + t_{II}}{t_{II}}$		Not possible if $t_I > 2$ and $t_{II} > 2$
S25	For every t_I and t_{II}		$T_{1I} = T_{D\min}; T_{1II} = \frac{1 + t_I}{t_{II}} T_{D\min}$

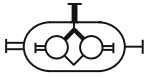
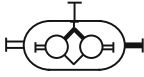
(continued)

Table 8.6 (continued)

Scheme	t_I and t_{II}	Structural symbol	T_{II} and $T_{I II} = f(t_I, t_{II}, T_{D \min})$
S26	For every t_I and t_{II}		$T_{II} = T_{D \min}; T_{I II} = (1 + t_I)T_{D \min}$
S33	$t_I \geq 2t_{II}$		$T_{II} = T_{I II} = \frac{1}{t_I} T_{D \min}$
	$t_{II} \leq t_I \leq 2t_{II}$		$T_{II} = T_{I II} = \frac{1}{t_I - t_{II}} T_{D \min}$
S34	For every t_I and t_{II}		$T_{II} = \frac{1+t_{II}}{t_{II}} T_{D \min}; T_{I II} = \frac{1}{t_{II}} T_{D \min}$
S35	For every t_I and t_{II}		$T_{II} = \frac{t_{II}}{1+t_{II}} T_{D \min}; T_{I II} = \frac{1}{1+t_{II}} T_{D \min}$
S36	$t_I \geq 1 + t_{II}$		$T_{II} = T_{I II} = \frac{1}{1+t_{II}} T_{D \min}$
	$t_I \leq 1 + t_{II}$		$T_{II} = T_{I II} = \frac{1}{t_I} T_{D \min}$
S44	$t_I \geq t_{II}$		$T_{II} = \frac{1+t_{II}}{t_I - t_{II}} T_{D \min}; T_{I II} = \frac{1+t_I}{t_I - t_{II}} T_{D \min}$
S45	$t_I \geq \frac{1+t_{II}}{t_{II}-1}$		$T_{II} = \frac{t_{II}}{1+t_I+t_{II}} T_{D \min}; T_{I II} = \frac{1+t_I}{1+t_I+t_{II}} T_{D \min}$
	$t_I \leq \frac{1+t_{II}}{t_{II}-1}$		$T_{II} = \frac{1}{t_I} T_{D \min}; T_{I II} = \frac{1+t_I}{t_I \cdot t_{II}} T_{D \min}$
S46	For every t_I and t_{II}		$T_{II} = \frac{1}{t_I} T_{D \min}; T_{I II} = \frac{1+t_I}{t_I} T_{D \min}$
S55	$t_I \geq t_{II}$		$T_{II} = \frac{t_{II}}{t_I - t_{II}} T_{D \min}; T_{I II} = \frac{t_I}{t_I - t_{II}} T_{D \min}$
S56	$t_I \geq \frac{2}{t_{II}-1}$		$T_{II} = \frac{1}{1+t_I} T_{D \min}; T_{I II} = \frac{t_I}{1+t_I} T_{D \min}$
	$t_I \leq \frac{2}{t_{II}-1}$		Not possible if $t_I > 2$ and $t_{II} > 2$

(continued)

Table 8.6 (continued)

Scheme	t_I and t_{II}	Structural symbol	T_{II} and $T_{III} = f(t_I, t_{II}, T_{D \min})$
S66	$t_I \geq 1 + 2 t_{II}$		$T_{II} = T_{III} = \frac{1}{1+t_{II}} T_{D \min}$
	$t_{II} \leq t_I \leq 1 + 2 t_{II}$		$T_{II} = T_{III} = \frac{1}{t_I-t_{II}} T_{D \min}$

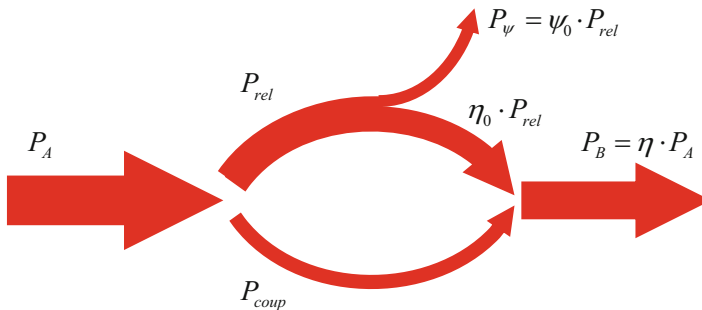


Fig. 8.7 Types of power in $\overline{\text{AI}}$ -PGT (Redrawn from [27])

$$T_1 \cdot \omega_{1 \text{ rel}} \begin{cases} > 0 & \text{— sun gear 1 is driving (input)} \\ < 0 & \text{— sun gear 1 is driven (output)} \end{cases} \quad (8.18)$$

Depending on the direction of the relative power, the real torques are determined as follows:

Driving (input) sun gear:

$$T'_3 = \eta_0 \cdot t \cdot T'_1 < T_3 \quad (8.19)$$

$$T'_1 = \frac{1}{\eta_0} \cdot \frac{T'_3}{t} > T_1 \quad (8.20)$$

Driven (output) sun gear:

$$T'_3 = \frac{1}{\eta_0} \cdot t \cdot T'_1 > T_3 \quad (8.21)$$

$$T'_1 = \eta_0 \cdot \frac{T'_3}{t} < T_1 \quad (8.22)$$

The correct determination of the torques can be easily checked by means of the equilibrium condition

$$T'_1 + T'_3 + T'_H = 0. \quad (8.23)$$

In the above formulae η_0 is the basic efficiency of the simple PGT in work with fixed carrier H

$$\eta_0 = 1 - \psi_0, \quad (8.24)$$

where ψ_0 is the basic loss factor.

For the purposes of first approximation comparative analysis, it is sufficient to assume some value of the basic efficiency $\eta_{0I} = \eta_{0II}$, the same for all Schemes [54]. However, when compiling computer programs, the influence of some factors on the basic efficiency can be taken into account. For example, [61] recommends determining the meshing loss factor by one of the known formulae [27], [63]

$$\psi_0 = (1 + k_B + k_S + k_C) \cdot \psi_{z_0} \quad (8.25)$$

where:

ψ_0 is the basic loss factor.

ψ_{z_0} is the meshing loss factor.

$k_B = 0.06 \div 0.07$ is the coefficient of planet bearing loss.

$k_S = 0.09 \div 0.01$ is the coefficient of sealing loss.

$k_C = 0.25 \div 0.02$ is the coefficient of churn and crushing loss.

The values on the left are for the high-speed stage [62].

With sufficient accuracy for engineering practice, meshing loss factor can be determined as follows [63]:

$$\psi_{z_0} = \frac{z_3 + z_1}{z_3 - z_1} \left(\frac{0.15}{z_1} + \frac{0.2}{z_3} \right). \quad (8.26)$$

On the basis of experimental studies [27, 64], it was found that in practice there is an equality of the meshing losses in $\overline{\text{AI}}$ -PGT (i.e., deviation of less than 5%), in the transmission of relative power P_{rel} from the sun gear 1 to the ring gear 3 and vice versa. This means

$$\psi_{z_{13(H)}} \approx \psi_{z_{31(H)}} = \psi_0 \quad (8.27)$$

For *basic efficiency* η_0 the following is obtained:

$$\eta_{13(H)} \approx \eta_{31(H)} = \eta_0 = 1 - \psi_0 \quad (8.28)$$

In order to be able to compare different structural schemes by efficiency, it is convenient to use their *aligned (reduced) efficiency* η_{red} , determined when working with a fixed summation shaft.

For all structural schemes from Table 8.1, the aligned (reduced) efficiency is determined as a function of the torque ratios t_I and t_{II} of the component PGTs and of their basic efficiencies η_{0I} and η_{0II}

$$\eta_{red} = f(t_I, t_{II}, \eta_{0I}, \eta_{0II}) \tag{8.29}$$

taking into account the change in the role of their shafts (Table 8.7).

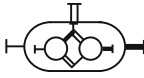


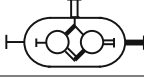
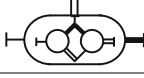
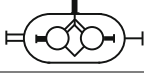
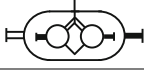
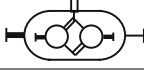
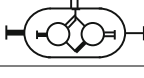
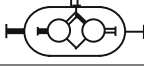
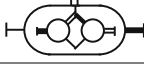
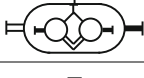
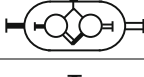
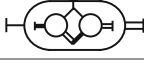
For the optimal choice of structural scheme by efficiency, it is sufficient to determine the scheme with the highest aligned (reduced) efficiency without looking for the efficiency at six cases of gear operation.

Table 8.7 Determination of the aligned efficiency η_{red} of structural schemes from Table 8.1 as a function of the torque ratios t_I and t_{II} and basic efficiencies η_{0I} and η_{0II} of the component PGTs (see t_{red} from Table 8.4)

Scheme	t_I and t_{II}	Structural symbol	$\eta_{0red} = f(t_I, t_{II}, \eta_{0I}, \eta_{0II})$
S11	$t_I \geq 2 t_{II}$		$\eta_{0red} = \frac{\frac{\eta_{0I} \cdot t_I}{1 - \eta_{0II}}}{\frac{t_I - \eta_{0II}}{t_I}}$
	$t_{II} \leq t_I \leq 2 t_{II}$		$\eta_{0red} = \frac{\frac{\eta_{0II} \cdot t_{II}}{t_I - \eta_{0II}}}{\frac{t_I - \eta_{0II}}{t_I}}$
S12	$t_I \geq 1 + t_{II}$		$\eta_{0red} = \frac{\frac{\eta_{0I} \cdot t_I}{1 + \eta_{0II}}}{\frac{t_I}{1 + t_{II}}}$
	$t_I \leq 1 + t_{II}$		$\eta_{0red} = \frac{\frac{1 + \eta_{0II} \cdot t_{II}}{t_I}}{\frac{t_I}{1 + t_{II}}}$
S13	For every t_I and t_{II}		$\eta_{0red} = \frac{\eta_{0I} \cdot \eta_{0II} \cdot t_I \cdot t_{II} - 1}{t_I \cdot t_{II} - 1}$
S14	For every t_I and t_{II}		$\eta_{0red} = \frac{\frac{\eta_{0I} \cdot \eta_{0II} \cdot t_I \cdot t_{II}}{1 + \eta_{0II} \cdot t_{II}}}{\frac{t_I \cdot t_{II}}{1 + t_{II}}}$
S15	For every t_I and t_{II}		$\eta_{0red} = \frac{\eta_{0I} \cdot t_I + \frac{\eta_{0I} \cdot t_I}{\eta_{0II}}}{t_I + \frac{t_I}{\eta_{0II}}}$
S16	For every t_I and t_{II}		$\eta_{0red} = \frac{\eta_{0I} \cdot t_I (1 + \eta_{0II} \cdot t_{II})}{t_I (1 + t_{II})}$
S22	$t_I \geq 1 + 2 t_{II}$		$\eta_{0red} = \frac{\frac{\eta_{0I} \cdot t_I}{1 + \eta_{0II}}}{\frac{t_I - \eta_{0II}}{1 + t_{II}}}$
	$t_{II} \leq t_I \leq 1 + 2 t_{II}$		$\eta_{0red} = \frac{\frac{1 + \eta_{0II} \cdot t_{II}}{t_I}}{\frac{t_I - \eta_{0II}}{1 + t_{II}}}$

(continued)

Table 8.7 (continued)

Scheme	t_I and t_{II}	Structural symbol	$\eta_{0red} = f(t_I, t_{II}, \eta_{0I}, \eta_{0II})$
S23	For every t_I and t_{II}		$\eta_{0red} = \frac{(1+\eta_{0I} \cdot t_I) \eta_{0II} \cdot t_{II}}{(1+t_I)t_{II}}$
S24	$t_I \geq \frac{2+t_{II}}{t_{II}}$		$\eta_{0red} = \frac{\eta_{0I} \cdot \eta_{0II} \cdot t_I \cdot t_{II} - 1}{t_I \cdot t_{II} - 1}$
	$t_I \leq \frac{2+t_{II}}{t_{II}}$		Not possible if $t_I > 2$ and $t_{II} > 2$
S25	For every t_I and t_{II}		$\eta_{0red} = \frac{1+\eta_{0I} \cdot t_I + \eta_{0I} \cdot \eta_{0II} \cdot t_I \cdot t_{II}}{\frac{\eta_{0II} \cdot t_{II}}{1+t_I+t_I \cdot t_{II}}}$
S26	For every t_I and t_{II}		$\eta_{0red} = \frac{\eta_{0I} \cdot t_I + \eta_{0II} \cdot t_{II} + \eta_{0I} \cdot \eta_{0II} \cdot t_I \cdot t_{II}}{t_I + t_{II} + t_I \cdot t_{II}}$
S33	$t_I \geq 2 t_{II}$		$\eta_{0red} = \frac{\frac{\eta_{0I} \cdot t_I}{t_I} - \frac{\eta_{II}}{\eta_{0II}}}{\frac{\eta_{0II}}{t_I - t_{II}}}$
	$t_{II} \leq t_I \leq 2 t_{II}$		$\eta_{0red} = \frac{\frac{\eta_{0II} \cdot t_{II}}{t_I} - \frac{\eta_{0I}}{\eta_{0II}}}{\frac{\eta_{II}}{t_I - t_{II}}}$
S34	For every t_I and t_{II}		$\eta_{0red} = \frac{\eta_{0I} \cdot t_I + \frac{\eta_{0II}}{t_{II}}}{t_I + \frac{1}{t_{II}}}$
S35	For every t_I and t_{II}		$\eta_{0red} = \frac{\eta_{0I} \cdot \eta_{0II} \cdot t_I \cdot t_{II}}{1 + \frac{\eta_{0II} \cdot t_{II}}{1+t_I}}$
S36	$t_I \geq 1 + t_{II}$		$\eta_{0red} = \frac{\frac{\eta_{0I} \cdot t_I}{1+t_{II}}}{\frac{\eta_{II}}{1+t_{II}}}$
	$t_I \leq 1 + t_{II}$		$\eta_{0red} = \frac{1 + \frac{\eta_{0II} \cdot t_{II}}{t_I}}{\frac{\eta_{II}}{1+t_{II}}}$
S44	$t_I \geq t_{II}$		$\eta_{0red} = \frac{\frac{\eta_{0II} \cdot t_{II}}{t_I} + \frac{\eta_{0II}}{\eta_{0I}} \cdot t_I \cdot t_{II}}{\frac{\eta_{II}}{t_{II} + t_I \cdot t_{II}}}$
S45	$t_I \geq \frac{1+t_{II}}{t_{II}-1}$		$\eta_{0red} = \frac{\eta_{0I} \cdot \eta_{0II} \cdot t_I \cdot t_{II}}{1 + \frac{\eta_{0I} \cdot t_I + \eta_{0II} \cdot t_{II}}{1+t_I+t_{II}}}$
	$t_I \leq \frac{1+t_{II}}{t_{II}-1}$		$\eta_{0red} = \frac{\frac{t_I}{1+t_{II}} + \frac{\eta_{II}}{\eta_{0II}}}{\frac{\eta_{0I} \cdot \eta_{0II}}{1+t_I+t_{II}}}$

(continued)

Table 8.7 (continued)

Scheme	t_I and t_{II}	Structural symbol	$\eta_{0red} = f(t_I, t_{II}, \eta_{0I}, \eta_{0II})$
S46	For every t_I and t_{II}		$\eta_{0red} = \frac{\frac{1+\eta_{0II} \cdot t_{II} \cdot \frac{\eta_{0II}}{\eta_{0I}} \cdot t_I \cdot \eta_{0I}}{\frac{\eta_{0I}}{\eta_{0II}}}}{\frac{1+t_{II} \pm t_I \cdot \eta_{0I}}{t_I}}$
S55	$t_I \geq t_{II}$		$\eta_{0red} = \frac{\frac{\eta_{0I} \cdot \eta_{0II} + \frac{\eta_{0II}}{\eta_{0I}} \cdot t_I \cdot \eta_{0I}}{\frac{t_I}{\eta_{0I}} - \eta_{0II} \cdot t_{II}}}{\frac{t_{II} \pm t_I \cdot \eta_{0I}}{t_I - t_{II}}}$
S56	$t_I \geq \frac{2}{t_{II}-1}$		$\eta_{0red} = \frac{\frac{\eta_{0I} \cdot \eta_{0II} \cdot t_I \cdot t_{II} - 1}{1 + \eta_{0II} \cdot t_{II}}}{\frac{t_I \cdot t_{II} - 1}{1 + t_I}}$
	$t_I \leq \frac{2}{t_{II}-1}$		Not possible if $t_I > 2$ and $t_{II} > 2$
S66	$t_{II} \geq 1 + 2 t_{II}$		$\eta_{0red} = \frac{\frac{\eta_{0I} \cdot t_I \cdot \frac{\eta_{0I}}{\eta_{0II}}}{1 + \frac{\eta_{0I}}{\eta_{0II}}}}{\frac{t_I - t_{II} - 1}{1 + t_{II}}}$
	$t_{II} \leq t_I \leq 1 + 2 t_{II}$		$\eta_{0red} = \frac{\frac{1 + \eta_{0II} \cdot t_{II}}{t_I} - \eta_{0II} \cdot t_{II}}{\frac{1 + t_{II}}{t_I - t_{II}}}$

8.2.2.3 Reduced Backlash

In some cases, the backlash in a PGT reduced to the input shaft may be important. The impact openings in reversing, for example, depend on it [65]. The same applies to the reduced stiffness.

In order to obtain comparable results for all structural schemes, the following simplification assumptions must be made:

- In all gears of all structural schemes, there is the same backlash (clearance) along the path of contact j'_z (Fig. 8.8).
- All gears are without profile shifting or modifications.
- All planet bearings are with the same radial clearance j_B .

From Fig. 8.8 it is seen that instead of a backlash along the path of contact j'_z it is possible to work with a backlash along the reference circle j_z , the relation between which can be assumed $j_z = j'_z \cdot \cos \alpha_w$ where α_w is the pressure angle.

Due to the clearances in the meshings and in the planet bearings, in PGT with two fixed shafts the third can rotate at an angle φ (φ_1 for sun gear, φ_3 for ring gear, and φ_H for carrier), which is the clearance reduced to the corresponding shaft (backlash).

If j'_{z12} is the backlash in the mesh of the sun gear 1 with the planets 2 and j'_{z23} is the backlash in the mesh of the planets 2 with the ring gear 3 (Figure 8.9a), it can be assumed that the tooth of the sun gear moves along the path of contact at a distance $j'_{z12} + j'_{z23} = 2 j'_z$. This is more convenient to express by moving along the reference circle $2 j_z$. Then because of the clearance in the bearings j_B , the tooth in question

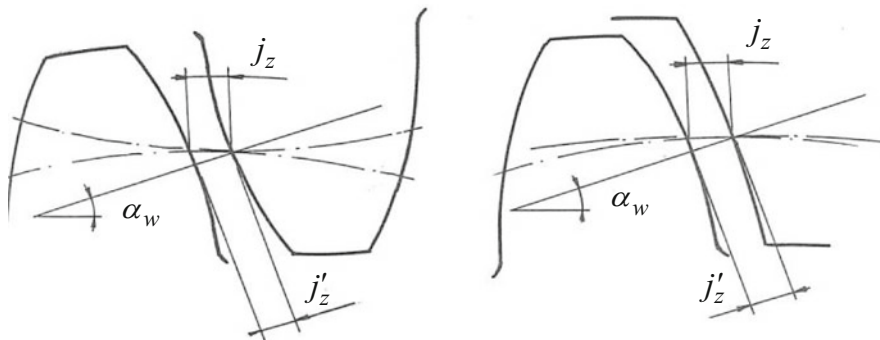


Fig. 8.8 Backlash in the meshing

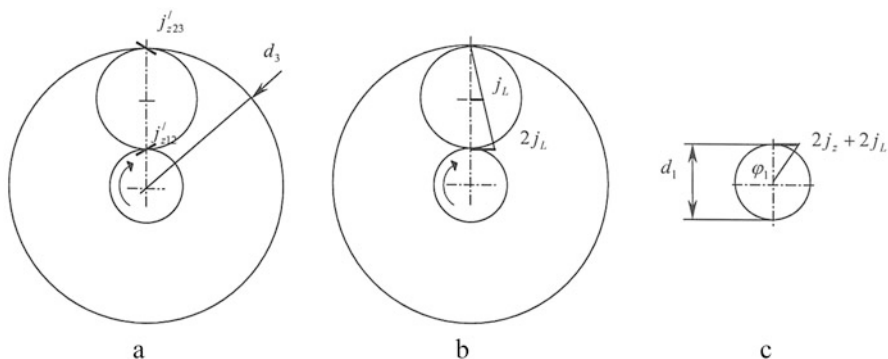


Fig. 8.9 Determination of the backlash of sun gear φ_1 in case of fixed ring gear 3 and carrier H (c) due the backlash in mesh (a) and the planet bearings clearance (b)

moves $2j_B$ along the reference circle (Fig. 8.9b). The all rotation of the sun gear φ_1 is determined in Figure 8.9c

$$\tan \varphi_1 = \frac{2j_z + 2j_B}{\frac{d_1}{2}} \tag{8.30}$$

The angle φ_1 is small enough to assume that $\varphi_1 = \tan \varphi_1$. Then the reduced backlash can be represented as follows:

$$\varphi_1 = \frac{4(j_z + j_B)}{d_1} \tag{8.31}$$

In a similar way, dependencies for the backlash reduced to the ring gear φ_3 and to the carrier φ_H can be obtained:

$$\varphi_3 = \frac{4(j_z + j_B)}{t \cdot d_1} = \frac{\varphi_1}{t} = i_{31(H)} \cdot \varphi_1, \tag{8.32}$$

$$\varphi_H = \frac{4(j_z + j_B)}{(1+t)d_1} = \frac{\varphi_1}{1+t} = i_{H1(3)} \cdot \varphi_1, \tag{8.33}$$

or

$$\varphi_H = \frac{t}{1+t} \varphi_3 = i_{H3(1)} \cdot \varphi_3. \tag{8.34}$$

Assuming that the output shaft is locked with a clearance allowing rotation (backlash) at an angle ξ_i , for each of the three above-considered cases, the reduced backlash can be determined by the formulae given in Table 8.8.

For the study of compound PGTs it is necessary to determine the reduced backlash taking into account the connections between the shafts of component PGTs.

Backlash reduced to a single external shaft (Fig. 8.10).

Firstly, the backlash φ_{bII} in the second PGT is determined, i.e., backlashes are reduced to the shaft *bII* forming the internal compound shaft *b*. Then the backlash φ_a of the input shaft is determined by the formulae in Table. 8.6; consider that $\xi_{bI} = \varphi_{bII}$.

Backlash reduced to a compound external shaft (Fig. 8.11).

In this case, the two component PGTs must be considered together. The rotation of the compound shaft can be represented as the sum of two angles

$$\varphi_d = \varphi'_d + \varphi^*_d, \tag{8.35}$$

where:

φ'_d is the angle (φ_{dI} or φ_{dII}) at which the backlash of one component PGT is completely removed.

φ^*_d is the angle at which the remaining backlash in the other PGT is removed.

The remaining backlash φ^*_d is removed simultaneously, both directly from the external compound shaft $\varphi_{d'}$ and through the internal compound shaft of the PGT whose backlash has already been removed $\varphi_{d''}$

$$\varphi^*_d = \frac{1}{\frac{1}{\varphi_{d'}} + \frac{1}{\varphi_{d''}}}. \tag{8.36}$$

For each structural scheme (Table 8.1) after applying the dependencies from (8.31) to (8.34) and from Table 8.6, by formulae (8.35) and (8.36) the backlashes reduced to the external compound shaft can be obtained.

Backlash reducing in a particle structural scheme

Determination of the backlash for structural scheme 15 from Table 8.1 is considered as an example, but the logic is the same for an arbitrary structural scheme.

Table 8.8 Reduced backlash to the input shaft φ_i in the case of output shaft locked with backlash ξ_i

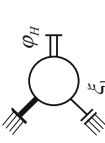

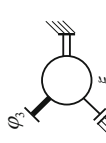

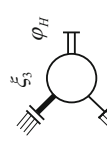

As a reducer (reduce the speed)		As a multiplier (multiply the speed)
	$\varphi_{1H} = \varphi_1 + i_{1H} \cdot \xi_H = \varphi_1 + (1 + t)\xi_H$	 $\varphi_{H1} = \varphi_H + i_{H1} \cdot \xi_1 = \varphi_H + \frac{1}{1+t}\xi_1$
	$\varphi_{13} = \varphi_1 + i_{13} \cdot \xi_3 = \varphi_1 + t \cdot \xi_3$	 $\varphi_{31} = \varphi_3 + i_{31} \cdot \xi_1 = \varphi_1 + \frac{1}{t}\xi_1$
	$\varphi_{3H} = \varphi_3 + i_{3H} \cdot \xi_H = \varphi_3 + \left(1 + \frac{1}{t}\right) \cdot \xi_H$	 $\varphi_{H3} = \varphi_H + i_{H3} \cdot \xi_3 = \varphi_H + \frac{1}{1+t}\xi_3$

Fig. 8.10 Backlash reduced to a single external shaft

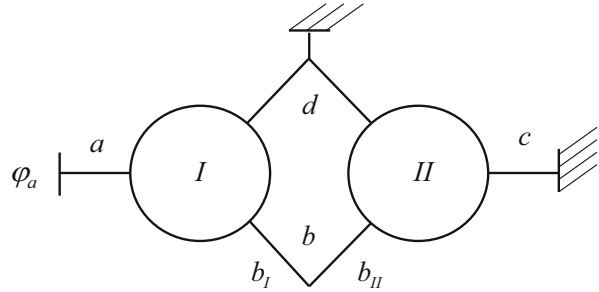
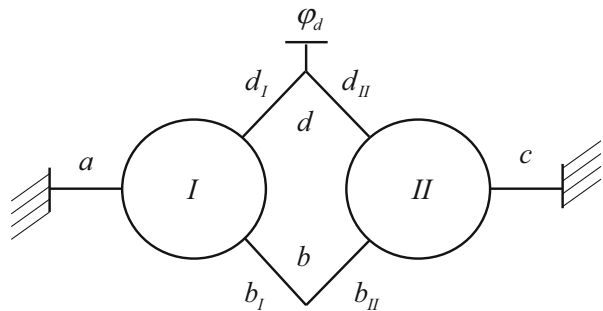


Fig. 8.11 Backlash reduced to a compound external shaft



Backlash reduced to the shaft a (Figure 8.12a)

The backlash in the second component PGT reduced to the ring gear is determined by formula (8.32)

$$\varphi_{3II} = \frac{4(j_z + j_B)}{t_{II} \cdot d_{1II}}. \tag{8.37}$$

The backlash in the first component PGT reduced to the sun gear at fixed carrier and locked with clearance $\xi_3 = \varphi_{3II}$ ring gear is determined by Table 8.6

$$\varphi_a = \varphi_{1I} + t_I \cdot \varphi_{3II}, \tag{8.38}$$

where:

φ_{1I} is the rotation of sun gear caused by clearances in the first PGT, determined by formula (8.31)

$$\varphi_{1I} = \frac{4(j_z + j_B)}{d_{1I}}. \tag{8.39}$$

After substitution in the corresponding formula in Table 8.6, for the reduced backlash the following is obtained:

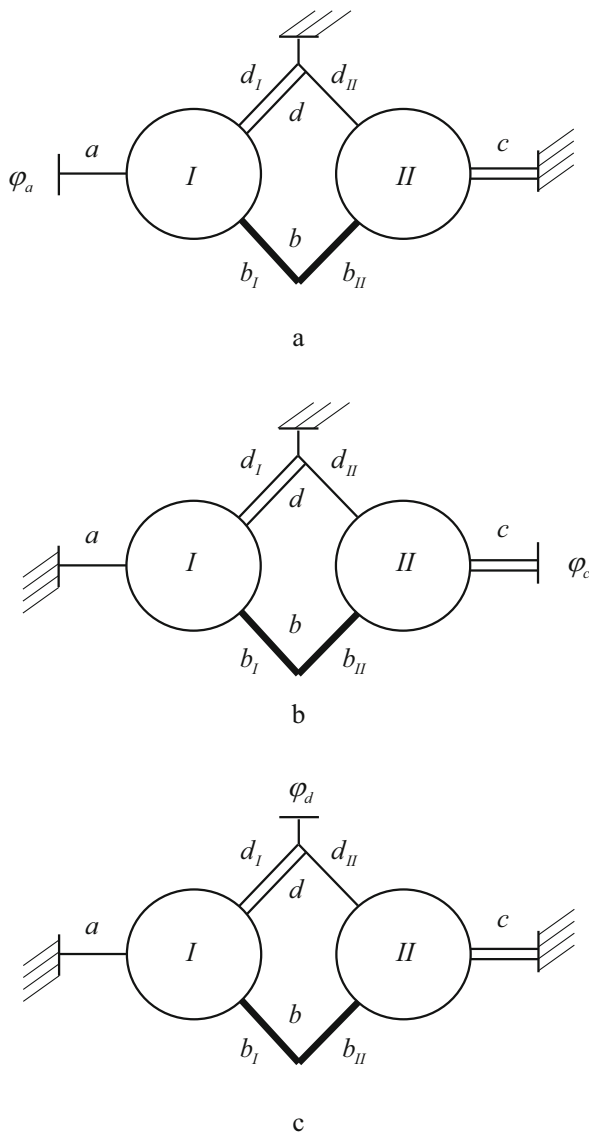


Fig. 8.12 Determination of reduced backlash in the compound two-carrier PGT arranged according to Scheme 15 from Table 8.1: (a) Backlash reduced to the single external shaft a . (b) Backlash reduced to the single external shaft c . (c) Backlash reduced to the compound external shaft d

$$\varphi_a = \frac{4(j_z + j_B)}{d_{1I}} + \frac{t_I}{t_{II}} \cdot \frac{4(j_z + j_B)}{d_{1II}}. \quad (8.40)$$

Backlash reduced to the shaft c (Figure 8.12b)

The backlash in the first component PGT reduced to the ring gear is determined by formula (8.32)

$$\varphi_{3I} = \frac{4(j_z + j_B)}{t_I \cdot d_{1I}}. \quad (8.41)$$

The backlash in the second component PGT reduced to the carrier at fixed sun gear and locked with clearance $\xi_3 = \varphi_{3I}$ ring gear is determined by Table 8.6:

$$\varphi_c = \varphi_{HII} + \frac{t_{II}}{1 + t_{II}} \cdot \varphi_{3I}, \quad (8.42)$$

where:

φ_{HII} is the rotation of carrier caused by clearances in the second PGT, determined by formula (8.24)

$$\varphi_{HII} = \frac{4(j_z + j_B)}{(1 + t_{II})d_{1II}}. \quad (8.43)$$

After substitution in the corresponding formula in Table 8.6, for the reduced backlash the following is obtained:

$$\varphi_c = \frac{4(j_z + j_B)}{(1 + t_{II})d_{1II}} + \frac{t_{II}}{1 + t_{II}} \cdot \frac{4(j_z + j_B)}{t_I \cdot d_{1I}}. \quad (8.44)$$

Backlash reduced to the shaft d (Figure 8.12c)

The backlashes in the two component PGTs, reduced to the shafts forming the compound one, are determined: reduced to the carrier of the first PGT by formula (8.33) and to the sun gear of the second PGT by formula (8.31)

$$\varphi_{dI} = \frac{4(j_z + j_B)}{(1 + t_I)d_{1I}}; \quad \varphi_{dII} = \frac{4(j_z + j_B)}{d_{1II}}. \quad (8.45)$$

In order to apply formula (8.35), it must be determined which of the two rotations is smaller (φ'_d). For this purpose, the sizes of the diameters of the sun gears must be determined by formula (8.15)

$$d_{1I} = K_0 \sqrt[3]{T_{1I} \frac{t_I + 1}{t_I - 1}}; \quad d_{1II} = K_0 \sqrt[3]{T_{1II} \frac{t_{II} + 1}{t_{II} - 1}}. \quad (8.46)$$

From the kinematic analysis and Table 8.5, it is known that for Scheme 15 T_{1I} is the smallest external torque and input torque, when operating as a reducer, i.e., $T_{1I} = T_{D\min} = T_A$, and T_{1II} is obtained as follows:

$$T_{1II} = \frac{t_I}{t_{II}} T_{1I}. \quad (8.47)$$

Substituting formula (8.47) into formula (8.46) for the sun gears diameters, the following is obtained:

$$d_{1I} = K_0 \sqrt[3]{T_{1I} \frac{t_I + 1}{t_I - 1}}, \quad d_{1II} = K_0 \sqrt[3]{T_{1I} \frac{t_I(t_{II} + 1)}{t_{II}(t_{II} - 1)}}. \quad (8.48)$$

After substituting formula (8.48) into formula (8.45) and comparing, it is established that for each t_I and $t_{II} \in [2 \div 12]$, the inequality $\varphi_{dI} > \varphi_{dII}$ is valid. Then the rotation of the input shaft by formula (8.35) is as follows:

$$\varphi_d = \varphi_{dI} + \varphi^*, \quad (8.49)$$

where φ^* is determined by formula (8.36)

$$\varphi_d^* = \frac{1}{\frac{1}{\varphi_d'} + \frac{1}{\varphi_d''}} \left| \begin{array}{l} \varphi_d' = \varphi_{dII} - \varphi_{dI} \\ \varphi_d'' = \frac{\varphi_d'}{t_{II}} i_{h3I} = \frac{\varphi_d'}{t_{II}} \cdot \frac{t_I}{1 + t_I} \end{array} \right. \quad (8.50)$$

After substitution for φ_d , the following is obtained:

$$\varphi_d = 4(j_z + j_B) \left[\left(\frac{1}{d_{1II}} - \frac{1}{(1 + t_I)d_{1I}} \right) \frac{t_I}{t_I + t_{II} + t_I \cdot t_{II}} + \frac{1}{(1 + t_I)d_{1I}} \right]. \quad (8.51)$$

After processing the formulae (8.40), (8.42), and (8.51), for the backlash reduced to the three external shafts, the following is obtained:

$$\varphi_a = 4(j_z + j_B) A_{15}, \quad (8.52)$$

$$\varphi_c = 4(j_z + j_B) A_{15} \frac{t_{II}}{t_I + t_I \cdot t_{II}}, \quad (8.53)$$

$$\varphi_d = 4(j_z + j_B) A_{15} \frac{t_{II}}{t_I + t_{II} + t_I \cdot t_{II}}, \quad (8.54)$$

where the constant A_{15} is

$$A_{15} = \frac{t_I \cdot d_{1I} + t_{II} \cdot d_{1II}}{t_{II} \cdot d_{1I} \cdot d_{1II}}. \quad (8.55)$$

From Table 8.4 it is seen that the aligned (reduced) torque ratio of Scheme 15 is

$$t_{red} = t_I + \frac{t_I}{t_{II}} = \frac{t_I + t_I \cdot t_{II}}{t_{II}}. \quad (8.56)$$

Then for the backlash reduced to the three outer shafts, it is

$$\varphi_a = 4(j_z + j_B)A_{15}, \quad (8.57)$$

$$\varphi_c = \frac{\varphi_a}{t_{red}}, \quad (8.58)$$

$$\varphi_d = \frac{\varphi_a}{1 + t_{red}}. \quad (8.59)$$

The constant A_{15} can be expressed as a function of the torque ratios (t_I and t_{II}) and the smallest of the torques on the external shafts $T_{D \min}$, which for this scheme is the torque of the shaft of the sun gear of the first component PGT ($T_{D \min} \equiv T_{1I}$)

$$A_{15} = \frac{t_I \sqrt[3]{\frac{t_I+1}{t_I-1}} + t_{II} \sqrt[3]{\frac{t_I(t_{II}+1)}{t_{II}(t_{II}-1)}}}{K_0 \cdot t_I \cdot t_{II} \sqrt[3]{T_{D \min} \frac{t_I(t_I+1)(t_{II}+1)}{t_{II}(t_I-1)(t_{II}-1)}}}. \quad (8.60)$$

Backlash reducing in structural schemes from Table 8.1

For each of the structural schemes from Table 8.1, the backlashes reduced to the three external shafts by the above procedure are determined. The constants A_{ij} analogous to those determined by formula (8.60) are determined. For each of the structural schemes, the below dependencies are valid:

$$\varphi_{D \min} = 4(j_z + j_B)A_{ij}, \quad (8.61)$$

$$\varphi_{D \max} = \frac{\varphi_{D \min}}{t_{red}}, \quad (8.62)$$

$$\varphi_{\Sigma} = \frac{\varphi_{D \min}}{1 + t_{red}}, \quad (8.63)$$

where:

$\varphi_{D \min}$ is the backlash reduced to the shaft with the smallest external torque $T_{D \min}$.

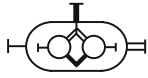
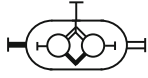
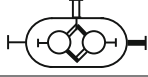
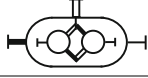
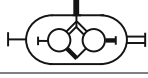
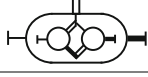
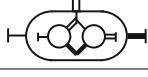
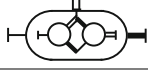
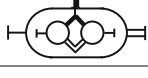
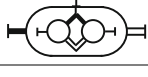
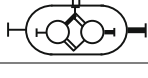
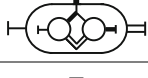

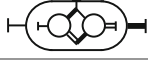
$\varphi_{D \max}$ is the backlash reduced to the shaft with the biggest external torque $T_{D \max}$.

φ_{Σ} is the backlash reduced to the shaft with summation external torque T_{Σ} .

A_{ij} is an original expression peculiar to each structural scheme (Table 8.9).

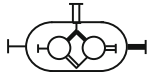
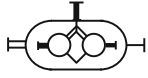
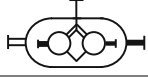
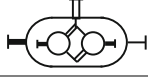
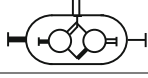
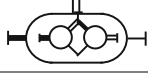
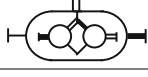
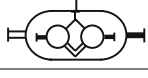
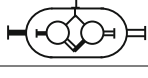
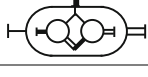
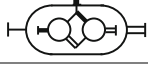
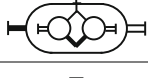
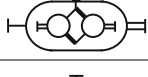
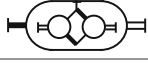
t_{red} is the aligned (reduced) speed ratio of compound PGT in question (Table 8.4).

Table 8.9 Determination of constant A_{ij} in formula (8.61).

Scheme	t_I and t_{II}	Structural symbol	$A_{ij} = f(t_I, t_{II}, d_{VI}, d_{VII})$
S11	$t_I \geq 2t_{II}$		$A_{11} = \frac{t_I \cdot d_{VI} + t_{II} \cdot d_{VII}}{t_{II} \cdot d_{VI} \cdot d_{VII}}$
	$t_{II} \leq t_I \leq 2t_{II}$		$A_{11} = \frac{t_I \cdot d_{VI} + t_{II} \cdot d_{VII}}{(t_I - t_{II})d_{VI} \cdot d_{VII}}$
S12	$t_I \geq 1 + t_{II}$		$A_{12} = \frac{t_I \cdot d_{VI} + (1 + t_{II})d_{VII}}{(1 + t_{II})d_{VI} \cdot d_{VII}}$
	$t_I \leq 1 + t_{II}$		$A_{12} = \frac{t_I \cdot d_{VI} + (1 + t_{II})d_{VII}}{t_I \cdot d_{VI} \cdot d_{VII}}$
S13	For every t_I and t_{II}		$A_{13} = A_{16} = \frac{t_I \cdot d_{VI} + d_{VII}}{d_{VI} \cdot d_{VII}}$
S14	For every t_I and t_{II}		$A_{14} = \frac{t_I \cdot d_{VI} + (1 + t_{II})d_{VII}}{(1 + t_{II})d_{VI} \cdot d_{VII}}$
S15	For every t_I and t_{II}		$A_{15} = \frac{t_I \cdot d_{VI} + t_{II} \cdot d_{VII}}{t_{II} \cdot d_{VI} \cdot d_{VII}}$
S16	For every t_I and t_{II}		$A_{16} = A_{13} = \frac{t_I \cdot d_{VI} + d_{VII}}{d_{VI} \cdot d_{VII}}$
S22	$t_I \geq 1 + 2t_{II}$		$A_{22} = \frac{(1 + t_I)d_{VI} + (1 + t_{II})d_{VII}}{(t_I - t_{II})d_{VI} \cdot d_{VII}}$
	$t_{II} \leq t_I \leq 1 + 2t_{II}$		$A_{22} = \frac{(1 + t_I)d_{VI} + (1 + t_{II})d_{VII}}{(t_I - t_{II})d_{VI} \cdot d_{VII}}$
S23	For every t_I and t_{II}		$A_{23} = A_{26} = \frac{(1 + t_I)d_{VI} + d_{VII}}{d_{VI} \cdot d_{VII}}$
S24	$t_I \geq \frac{2 + t_{II}}{t_{II}}$		$A_{24} = \frac{(1 + t_I)d_{VI} + (1 + t_{II})d_{VII}}{(1 + t_{II})d_{VI} \cdot d_{VII}}$
	$t_I \leq \frac{2 + t_{II}}{t_{II}}$		Not possible if $t_I > 2$ and $t_{II} > 2$
S25	For every t_I and t_{II}		$A_{25} = \frac{(1 + t_I)d_{VI} + t_{II} \cdot d_{VII}}{t_{II} \cdot d_{VI} \cdot d_{VII}}$

(continued)

Table 8.9 (continued)

Scheme	t_I and t_{II}	Structural symbol	$A_{ij} = f(t_I, t_{II}, d_{VI}, d_{VII})$
S26	For every t_I and t_{II}		$A_{26} = A_{23} = \frac{(1 + t_I)d_{VI} + d_{VII}}{d_{VI} \cdot d_{VII}}$
S33	$t_I \geq 2t_{II}$		$A_{33} = \frac{d_{VI} + d_{VII}}{t_{II} \cdot d_{VI} \cdot d_{VII}}$
	$t_{II} \leq t_I \leq 2t_{II}$		$A_{33} = \frac{d_{VI} + d_{VII}}{(t_I - t_{II})d_{VI} \cdot d_{VII}}$
S34	For every t_I and t_{II}		$A_{34} = \frac{d_{VI} + (1 + t_{II})d_{VII}}{t_{II} \cdot d_{VI} \cdot d_{VII}}$
S35	For every t_I and t_{II}		$A_{35} = \frac{d_{VI} + t_{II} \cdot d_{VII}}{(1 + t_{II})d_{VI} \cdot d_{VII}}$
S36	$t_I \geq 1 + t_{II}$		$A_{36} = \frac{d_{VI} + d_{VII}}{(1 + t_{II})d_{VI} \cdot d_{VII}}$
	$t_I \leq 1 + t_{II}$		$A_{36} = \frac{d_{VI} + d_{VII}}{t_I \cdot d_{VI} \cdot d_{VII}}$
S44	$t_I \geq t_{II}$		$A_{44} = \frac{(1 + t_I)d_{VI} + (1 + t_{II})d_{VII}}{(t_I - t_{II})d_{VI} \cdot d_{VII}}$
S45	$t_I \geq \frac{1 + t_{II}}{t_{II} - 1}$		$A_{45} = \frac{(1 + t_I)d_{VI} + t_{II} \cdot d_{VII}}{(1 + t_I + t_{II})d_{VI} \cdot d_{VII}}$
	$t_I \leq \frac{1 + t_{II}}{t_{II} - 1}$		$A_{45} = \frac{(1 + t_I)d_{VI} + t_{II} \cdot d_{VII}}{t_I \cdot t_{II} \cdot d_{VI} \cdot d_{VII}}$
S46	For every t_I and t_{II}		$A_{46} = \frac{(1 + t_I)d_{VI} + d_{VII}}{t_I \cdot d_{VI} \cdot d_{VII}}$
S55	$t_I \geq t_{II}$		$A_{46} = \frac{(1 + t_I)d_{VI} + d_{VII}}{t_I \cdot d_{VI} \cdot d_{VII}}$
S56	$t_I \geq \frac{2}{t_{II} - 1}$		$A_{56} = \frac{t_I \cdot d_{VI} + d_{VII}}{(1 + t_I)d_{VI} \cdot d_{VII}}$
	$t_I \leq \frac{2}{t_{II} - 1}$		Not possible if $t_I > 2$ and $t_{II} > 2$

(continued)

Table 8.9 (continued)

Scheme	t_I and t_{II}	Structural symbol	$A_{ij} = f(t_I, t_{II}, d_{1I}, d_{1II})$
S66	$t_I \geq 1 + 2t_{II}$		$A_{66} = \frac{d_{1I} + d_{1II}}{(1 + t_{II})d_{1I} \cdot d_{1II}}$
	$t_{II} \leq t_I \leq 1 + 2t_{II}$		$A_{66} = \frac{d_{1I} + d_{1II}}{(t_I - t_{II})d_{1I} \cdot d_{1II}}$

8.2.2.4 Reduced Stiffness

Sometimes it is important to know the dynamic parameters of the transmission, including the gear train. In this case, it is advisable to take into account the possible dynamic characteristics when choosing the structural scheme. In order to study the influence of the structural scheme and its parameters on the reduced to the external shafts’ stiffness of the PGT, the shafts can be considered as perfectly rigid, and only the stiffnesses in the gearing and planet bearings can be taken into account. The analysis of real arrangements shows that the angular compliance of the shafts is not more than 5 to 10% of the compliance of the gear train [66].

It is convenient to present the stiffness in the meshing as follows [54]:

$$c_z = \frac{F_{bn}}{\Delta_z}, \tag{8.64}$$

where:

c_z is the mean value of mesh stiffness, $\frac{N}{\mu m}$.

Δ_z is the tooth deformation on the path of contact, μm .

F_{bn} is the normal load (force) in the mesh, N.

Normal force can be represented as

$$F_{bn} = \frac{2T}{d_w \cdot \cos \alpha_w}, \tag{8.65}$$

where:

T is the torque on the shaft of one of the mated gears, N.

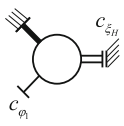
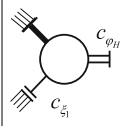
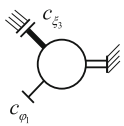
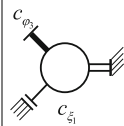
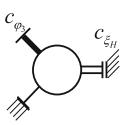
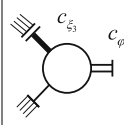
d_w is the diameter of operating circle of the gear in question. For gears without profile shifting, it is equal to the reference diameter ($d_w = d$), m.

α_w is the pressure angle.

The angle of rotation of the shaft of gear in question due to deformation Δ_c can be represented as

$$\varphi_c \approx \tan \varphi_c = \frac{2\Delta_c \cdot \cos \alpha_w}{d}. \tag{8.66}$$

Table 8.10 Reduced stiffness to the input shaft c_φ in the case of output shaft locked with stiffness c_ξ

As a reducer (reduce the speed)		As a multiplier (multiply the speed)	
	$c_{\varphi_{1H}} = \frac{1}{\frac{1}{c_{\varphi_1}} + (1+t)^2 \frac{1}{c_{\xi_H}}}$		$c_{\varphi_{H1}} = \frac{1}{\frac{1}{c_{\varphi_H}} + \frac{1}{(1+t)^2} \cdot \frac{1}{c_{\xi_1}}}$
	$c_{\varphi_{13}} = \frac{1}{\frac{1}{c_{\varphi_1}} + t^2 \frac{1}{c_{\xi_3}}}$		$c_{\varphi_{31}} = \frac{1}{\frac{1}{c_{\varphi_3}} + \left(\frac{1}{t}\right)^2 \frac{1}{c_{\xi_1}}}$
	$c_{\varphi_{3H}} = \frac{1}{\frac{1}{c_{\varphi_3}} + \left(1 + \frac{1}{t}\right)^2 \frac{1}{c_{\xi_H}}}$		$c_{\varphi_{H3}} = \frac{1}{\frac{1}{c_{\varphi_H}} + \frac{1}{\left(1 + \frac{1}{t}\right)^2} \cdot \frac{1}{c_{\xi_3}}}$

After substitution of formulae (8.64) and (8.65) in (8.66), the angular rotation of the shaft is obtained:

$$\varphi_c = \frac{4T}{c_z \cdot d^2}. \tag{8.67}$$

Then the angular stiffness $c_\varphi = \frac{T}{\varphi_c}$ is equal to

$$c_\varphi = \frac{c_z \cdot d^2}{4}. \tag{8.68}$$

After reasoning similar to those for backlashes (Sect. 2.2.3), dependencies for the stiffness reduced to the three shafts of a simple PGT with one fixed shaft and one locked with stiffness can be created (Table 8.10) [54].

Based on these dependencies, the reduced stiffness to the input shaft (external shaft with the lowest torque $T_{D \min}$) of the compound PGT can be determined. For compound PGTs in Table 8.4, the formula is [54].

$$c_{\varphi_{D \min}} = \frac{k}{8 \left(\frac{1}{c_z} + \frac{1}{c_B}\right) B_{ij}}, \tag{8.69}$$

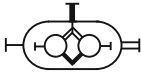
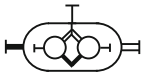

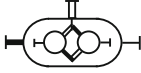
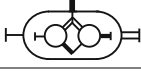
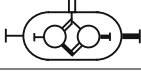
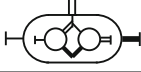
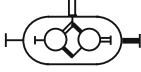

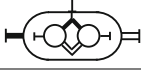
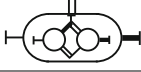


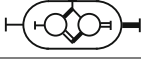
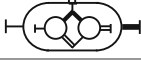
where:

k is the number of planets.

c_z and c_B are the stiffnesses in the mesh and planet bearings.

$B_{ij} = f(t_I, t_{II}, d_{1I}, d_{1II})$ is an original expression peculiar to each structural scheme (Table 8.11).

Table 8.11 Determination of constant B_{ij} in formula (8.69)

Scheme	t_I and t_{II}	Structural symbol	$B_{ij} = f(t_I, t_{II}, d_{1I}, d_{1II})$
S11	$t_I \geq 2 t_{II}$		$B_{11} = \frac{t_I^2 \cdot d_{1I}^2 + t_{II}^2 \cdot d_{1II}^2}{t_I^2 \cdot d_{1I}^2 \cdot d_{1II}^2}$
	$t_{II} \leq t_I \leq 2 t_{II}$		$B_{11} = \frac{t_I^2 \cdot d_{1I}^2 + t_{II}^2 \cdot d_{1II}^2}{(t_I^2 - t_{II}^2) d_{1I}^2 \cdot d_{1II}^2}$
S12	$t_I \geq 1 + t_{II}$		$B_{12} = \frac{t_I^2 \cdot d_{1I}^2 + (1+t_{II})^2 \cdot d_{1II}^2}{(1+t_{II})^2 \cdot d_{1I}^2 \cdot d_{1II}^2}$
	$t_I \leq 1 + t_{II}$		$B_{12} = \frac{t_I^2 \cdot d_{1I}^2 + (1+t_{II})^2 \cdot d_{1II}^2}{t_I^2 \cdot d_{1I}^2 \cdot d_{1II}^2}$
S13	For every t_I and t_{II}		$B_{13} = B_{16} = \frac{t_I^2 \cdot d_{1I}^2 + d_{1II}^2}{d_{1I}^2 \cdot d_{1II}^2}$
S14	For every t_I and t_{II}		$B_{14} = \frac{t_I^2 \cdot d_{1I}^2 + (1+t_{II})^2 \cdot d_{1II}^2}{(1+t_{II})^2 \cdot d_{1I}^2 \cdot d_{1II}^2}$
S15	For every t_I and t_{II}		$B_{15} = \frac{t_I^2 \cdot d_{1I}^2 + t_{II}^2 \cdot d_{1II}^2}{t_I^2 \cdot d_{1I}^2 \cdot d_{1II}^2}$
S16	For every t_I and t_{II}		$B_{16} = B_{13} = \frac{t_I^2 \cdot d_{1I}^2 + d_{1II}^2}{d_{1I}^2 \cdot d_{1II}^2}$
S22	$t_I \geq 1 + 2 t_{II}$		$B_{22} = \frac{(1+t_I)^2 \cdot d_{1I}^2 + (1+t_{II})^2 \cdot d_{1II}^2}{(t_I^2 - t_{II}^2) d_{1I}^2 \cdot d_{1II}^2}$
	$t_{II} \leq t_I \leq 1 + 2 t_{II}$		$B_{22} = \frac{(1+t_I)^2 \cdot d_{1I}^2 + (1+t_{II})^2 \cdot d_{1II}^2}{(t_I^2 - t_{II}^2) d_{1I}^2 \cdot d_{1II}^2}$
S23	For every t_I and t_{II}		$B_{23} = B_{26} = \frac{(1+t_I)^2 \cdot d_{1I}^2 + d_{1II}^2}{d_{1I}^2 \cdot d_{1II}^2}$
S24	$t_I \geq \frac{2+t_{II}}{t_{II}}$		$B_{24} = \frac{(1+t_I)^2 \cdot d_{1I}^2 + (1+t_{II})^2 \cdot d_{1II}^2}{(1+t_{II})^2 \cdot d_{1I}^2 \cdot d_{1II}^2}$
	$t_I \leq \frac{2+t_{II}}{t_{II}}$		Not possible if $t_I > 2$ and $t_{II} > 2$
S25	For every t_I and t_{II}		$B_{25} = \frac{(1+t_I)^2 \cdot d_{1I}^2 + t_{II}^2 \cdot d_{1II}^2}{t_{II}^2 \cdot d_{1I}^2 \cdot d_{1II}^2}$
S26	For every t_I and t_{II}		$B_{26} = B_{23} = \frac{(1+t_I)^2 \cdot d_{1I}^2 + d_{1II}^2}{d_{1I}^2 \cdot d_{1II}^2}$

(continued)

Table 8.11 (continued)

Scheme	t_I and t_{II}	Structural symbol	$B_{ij} = f(t_I, t_{II}, d_{1I}, d_{1II})$
S33	$t_I \geq 2t_{II}$		$B_{33} = \frac{d_{1I}^2 + d_{1II}^2}{t_I^2 \cdot d_{1I}^2 \cdot d_{1II}^2}$
	$t_{II} \leq t_I \leq 2t_{II}$		$B_{33} = \frac{d_{1I}^2 + d_{1II}^2}{(t_I^2 - t_{II}^2) d_{1I}^2 \cdot d_{1II}^2}$
S34	For every t_I and t_{II}		$B_{34} = \frac{d_{1I}^2 + (1+t_{II})^2 d_{1II}^2}{t_I^2 \cdot d_{1I}^2 \cdot d_{1II}^2}$
S35	For every t_I and t_{II}		$B_{35} = \frac{d_{1I}^2 + t_{II}^2 \cdot d_{1II}^2}{(1+t_{II})^2 \cdot d_{1I}^2 \cdot d_{1II}^2}$
S36	$t_I \geq 1 + t_{II}$		$B_{36} = \frac{d_{1I}^2 + d_{1II}^2}{(1+t_{II})^2 \cdot d_{1I}^2 \cdot d_{1II}^2}$
	$t_I \leq 1 + t_{II}$		$B_{36} = \frac{d_{1I}^2 + d_{1II}^2}{t_I^2 \cdot d_{1I}^2 \cdot d_{1II}^2}$
S44	$t_I \geq t_{II}$		$B_{44} = \frac{(1+t_I)^2 \cdot d_{1I}^2 + (1+t_{II})^2 \cdot d_{1II}^2}{(t_I^2 - t_{II}^2) d_{1I}^2 \cdot d_{1II}^2}$
S45	$t_I \geq \frac{1+t_{II}}{t_{II}-1}$		$B_{45} = \frac{(1+t_I)^2 \cdot d_{1I}^2 + t_{II}^2 \cdot d_{1II}^2}{(1+t_I^2 + t_{II}^2) d_{1I}^2 \cdot d_{1II}^2}$
	$t_I \leq \frac{1+t_{II}}{t_{II}-1}$		$B_{45} = \frac{(1+t_I)^2 \cdot d_{1I}^2 + t_{II}^2 \cdot d_{1II}^2}{t_I^2 \cdot t_{II}^2 \cdot d_{1I}^2 \cdot d_{1II}^2}$
S46	For every t_I and t_{II}		$B_{46} = \frac{(1+t_I)^2 \cdot d_{1I}^2 + d_{1II}^2}{t_I^2 \cdot d_{1I}^2 \cdot d_{1II}^2}$
S55	$t_I \geq t_{II}$		$B_{55} = \frac{t_I^2 \cdot d_{1I}^2 + t_{II}^2 \cdot d_{1II}^2}{(t_I^2 - t_{II}^2) d_{1I}^2 \cdot d_{1II}^2}$
S56	$t_I \geq \frac{2}{t_{II}-1}$		$B_{56} = \frac{t_I^2 \cdot d_{1I}^2 + d_{1II}^2}{(1+t_I)^2 \cdot d_{1I}^2 \cdot d_{1II}^2}$
	$t_I \leq \frac{2}{t_{II}-1}$		Not possible if $t_I > 2$ and $t_{II} > 2$
S66	$t_I \geq 1 + 2t_{II}$		$B_{66} = \frac{d_{1I}^2 + d_{1II}^2}{(1+t_{II})^2 \cdot d_{1I}^2 \cdot d_{1II}^2}$
	$t_{II} \leq t_I \leq 1 + 2t_{II}$		$B_{66} = \frac{d_{1I}^2 + d_{1II}^2}{(t_I^2 - t_{II}^2) d_{1I}^2 \cdot d_{1II}^2}$

If the reference diameters of the sun gears are determined by formula (8.15) and Table 8.5, a formula can be obtained for the stiffnesses as a function of torque ratios t_I and t_{II} of the component PGTs and several constants: the stiffnesses in the mesh c_z and bearings c_B ; the number of planets k ; meshing parameters (K_0); and the input torque $T_A \equiv T_{D \min}$ (which affects the geometric dimensions).

By varying the values of t_I and t_{II} (in the range from 2 to 12), their influence on the reduced angular stiffness c_φ can be determined. From this one can look for the most favorable combination of t_I and t_{II} (i.e., the distribution of the total speed ratio between the two planetary stages) to obtain the desired stiffness. Also it is possible to make a comparative analysis between the different structural schemes. It is appropriate to emphasize that of the above optimization criteria, the reduced stiffness is the least important for the choice of the structural scheme and its parameters. In many of the mechanisms in the transmission or in the working body, there are quite large elasticities (couplings, ropes, chains, pneumatic wheels, etc.), which minimize the impact of the elasticity of the gear.

In multi-objective optimization, other parameters can be defined (e.g., gear trains mass).

8.2.3 Multi-Objective Optimization Procedure

8.2.3.1 Optimization within One Structural Scheme

The given required total speed ratio of the compound PGT, resp. the aligned torque ratio t_{red} , can be realized at different values of the torque ratios t_I and t_{II} of the component PGTs. The purpose of optimization is to find the most suitable combination.

One of the possible approaches is to vary the values of t_I and t_{II} in a certain interval (for the considered PGT it is from 2 to 12). The variation step can be chosen small enough (e.g., 0.1) without being related to the number of teeth on the sun wheel and the ring gear (to facilitate the procedure) [54]. If desired, the number of teeth can be included by setting a value for and increasing by one tooth [49].

For each of the combinations of t_I and t_{II} , the values of the parameters used for optimization criteria are determined (ring gears diameters d_{3I} and d_{3II} , efficiency η_{red} , the reduced backlash to the input shaft $\varphi_{D \min}$). Then, by one of the known methods for multi-objective optimization, the most appropriate combination is chosen.

The case of Pareto optimization by weight coefficients [67, 68] is presented below, which the authors consider the most appropriate in this case. Other methods are also possible [69].

In [42] programs for optimal choice of the torque ratios of the component gear trains t_I and t_{II} from the standpoint of maximum efficiency and minimum overall dimensions and backlash are proposed for each of the possible structural schemes (Tables 8.1 and 8.2). All these programs contain a module which determines whether

the structural scheme has the required kinematic capabilities when changing t_I and t_{II} within a given interval in order to fulfill:

- The desired value for speed ratio $i = \frac{\omega_A}{\omega_B}$, i.e., for aligned (reduced) torque ratio of compound PGT t_{red} in case of PGT from Table 8.1.
- The desired values for the two output angular velocities ω_B and $\omega_{B\mu}$ in case of PGT from Table 8.2.
- A desired ratio between the two output angular velocities $\frac{\omega_B}{\omega_{B\mu}}$ in case of PGT from Table 8.2.

The range of t_I and t_{II} is chosen by the user and cannot go out of the previously determined values

$$2 \leq t_{I \min} \leq t_I \leq t_{I \max} \leq 12 \quad (8.70)$$

$$2 \leq t_{II \min} \leq t_{II} \leq t_{II \max} \leq 12. \quad (8.71)$$

For the structural schemes of the main diagonal of Tables 8.1 and 8.2, this check is connected with the minimum allowed values for the efficiency

$$\eta_{Br.1} \geq \eta_{\min} \quad \text{and} \quad \eta_{Br.2} \geq \eta_{\min} \quad (8.72)$$

as if $t_I = t_{II}$ in theory infinity is obtained for the speed ratio and zero for the efficiency.

The above check for the kinematic capabilities could be made by directly assigning values to t_I and t_{II} at regular intervals with no connection to a certain number of teeth.

The efficiency of the component gear train is a function of the torque ratios t_I and t_{II} and the basic efficiencies η_{OI} and η_{OII} of the component PGTs. For a more accurate reading of the influence of the structural scheme parameters on the efficiency, an approach is assumed, in which the efficiencies of the component PGTs η_{OI} and η_{OII} are determined as a function of the number of teeth of the gears in the corresponding PGT [63]

$$\eta_0 = 1 - \psi_z = 1 - \frac{z_3 + z_1}{z_3 - z_1} \left(\frac{0,15}{z_1} + \frac{0,2}{z_3} \right). \quad (8.73)$$

For this reason the following approach for determining t_I and t_{II} is used:

1. Choice of number of teeth for the sun gears of the component gear trains z_{1I} and z_{1II} .
2. Determination of minimum and maximum number of teeth of the ring gears $z_{3I} \min = t_I \min \cdot z_{1I}$, $z_{3II} \min = t_{II} \min \cdot z_{1II}$, $z_{3I} \max = t_I \max \cdot z_{1I}$, $z_{3II} \max = t_{II} \max \cdot z_{1II}$.
3. Determination of the current values of the torque ratios $t_I = \frac{z_{3I}}{z_{1I}}$ and $t_{II} = \frac{z_{3II}}{z_{1II}}$.

4. Consecutive increase in the number of teeth of the ring gear of one gear train (e.g., the second one) one tooth at a time until the maximum value (determined in p. 2) is reached.
5. Consecutive increase in the number of teeth of the other gear train (e.g., the first one) one tooth at a time, while the cycle is repeated for the second gear train (p. 3) until the maximum value (determined in p. 2) is reached.

The program allows the inclusion of fulfillment check for the additional conditions when choosing the number of teeth:

- Coaxiality condition, i.e.,

$$z_2 = \frac{z_3 - z_1}{2} = \text{int} \quad (8.74)$$

- Mounting condition

$$\frac{z_3 + z_1}{k} = \text{int} \quad (8.75)$$

In practice, the coaxiality condition is eluded by choosing appropriate corrections of the tooth meshing, which are even recommended from the standpoint of teeth bending stiffness.

The mounting condition could also be eluded [27] with appropriate design solutions.

A program is created, which determines within 3 cycles the current values of the various parameters of the component (η_{0I} , η_{0II} , d_{3I} , d_{3II}) and compound (η_{0red} , $\varphi_{D\min}$, $\eta_{Br.1}$, $\eta_{Br.2}$, $\varphi_{Br.1}$, $\varphi_{Br.2}$) planetary gear trains as a function of t_I and t_{II} .

The thus established database is used for building the graphical relations of the changes in the parameters as a function of t_I and t_{II} , which contribute to the quick orientation of the designer in the capabilities of the various structural schemes.

Due to differences in the dimensions and variations of the individual criteria, they are normalized while nondimensional quantitative measures are assumed:

$$k_i(t_I, t_{II}) = \frac{f_i(t_I, t_{II}) - f_i^{\min}}{f_i^{\max} - f_i^{\min}}$$

or

$$k_j(t_I, t_{II}) = \frac{f_j^{\max} - f_j(t_I, t_{II})}{f_j^{\max} - f_j^{\min}} \quad (8.76)$$

where:

$k_i(t_I, t_{II})$ is the normalized (nondimensional) value of the criteria with minimum values.

$k_j(t_I, t_{II})$ is the normalized (nondimensional) value of the criteria with maximum values.

$f_i(t_I, t_{II})$ and $f_j(t_I, t_{II})$ are the current values of the corresponding characteristics.

f_{\max} and f_{\min} are the extremal values of the characteristics in the given range of t_I and t_{II} .

The generalized criterion is assigned. It is expressed by a purpose function obtained from the scalar product of the vectors, the components of which are weight coefficients and nondimensional purpose evaluations

$$Z(t_I, t_{II}) = \sum_{i=1}^n \chi_i \cdot k_i(t_I, t_{II}) \quad (8.77)$$

where:

$\chi = (\chi_i)'$ is the vector of the weight coefficients, $0 < \chi_i < 1$; $\sum \chi_i = 1$.

$k = (k_i)'$ is the vector of the nondimensional purpose evaluations

$$(t_I^*, t_{II}^*) : \min_{t_{\min} \leq t_I, t_{II} \leq t_{\max}} Z(t_I, t_{II}). \quad (8.78)$$

The weight coefficients reflect the priority of each criterion. Thus, the different degree of importance of the various criteria for each particular case of gear train application is taken into account.¹

The optimal solution regarding the controlling parameters t_I and t_{II} is the one in which the purpose function (8.77) reaches its minimum value.

8.2.3.2 Optimal Choice of a Structural Scheme

Within the single-objective optimizations, the choice of the most appropriate structural scheme is reduced to the determination of the best combination of t_I and t_{II} for the chosen parameter in the various structural schemes, comparison of the parameter values, and determination of the most appropriate structural scheme (with the corresponding values of t_I and t_{II}).

In multi-objective optimization the most appropriate values for t_I and t_{II} for each of the given structural schemes are determined as well from the standpoint of the generalized criterion (8.77).

¹At the end of the twentieth century, there was a tendency toward dismissing the optimization methods with weight coefficients as subjective. Modern computer technology with its advanced dialogue mode enables the rapid simulation of different variants (with different weight coefficients) and renders these methods more flexible and suitable for various tasks, which definitely compensates the shortcomings of subjectivism and even turns it into advantage.

With first approximation one could expect the best structural scheme to be the one with the lowest value of the purpose function (8.77). For more accurate results, however, it is desirable that what is determined by the multi-objective optimization values of the individual criteria (characteristics, indices) be compared with one another. This means another normalization where (8.76) becomes

$$k_i(p_{sh}) = \frac{f_i(p_{sh}) - f_i^{\min}}{f_i^{\max} - f_i^{\min}}$$

or

$$k_j(p_{sh}) = \frac{f_j^{\max} - f_j(p_{sh})}{f_j^{\max} - f_j^{\min}} \quad (8.79)$$

where:

$k_i(p_{sh})$ is the normalized (nondimensional) value of the criteria with minimum values.

$k_j(p_{sh})$ is the normalized (nondimensional) value of the criteria with maximum values.

$f_i(p_{sh})$ and $f_j(p_{sh})$ are the current values of the corresponding characteristics obtained by multi-objective optimization of the various schemes.

f_{\max} and f_{\min} are the extremal values of the characteristics obtained by multi-objective optimization of the various schemes.

p_{sh} is the number of the structural scheme participating in the optimization.

The procedure for determining the purpose function (8.77) and its minimum value (8.78) is repeated for the thus determined nondimensional values of the criteria $k(p_{sh})$.

The process in (8.79) features the various versions of the structural schemes corresponding to the kinematic criterion (to provide the necessary ratio between the output angular velocities $\frac{\omega_B}{\omega_{B\mu}}$ in the admissible range of t_I and t_{II}).

Figure 8.13 presents the result of the optimization of all variants which provide the desired speed ratios (the most appropriate structural scheme is given in the bottom row).

The design, technological, and economic optimization methods reviewed in Sect. 1.1 can be applied to the variant chosen by the method above (according to the specific case).

A major advantage of the proposed program is the possibility to take different indices and study their dependence on the torque ratios of the component gear trains. This enables the detailed study of the various structural schemes (Fig. 8.14).

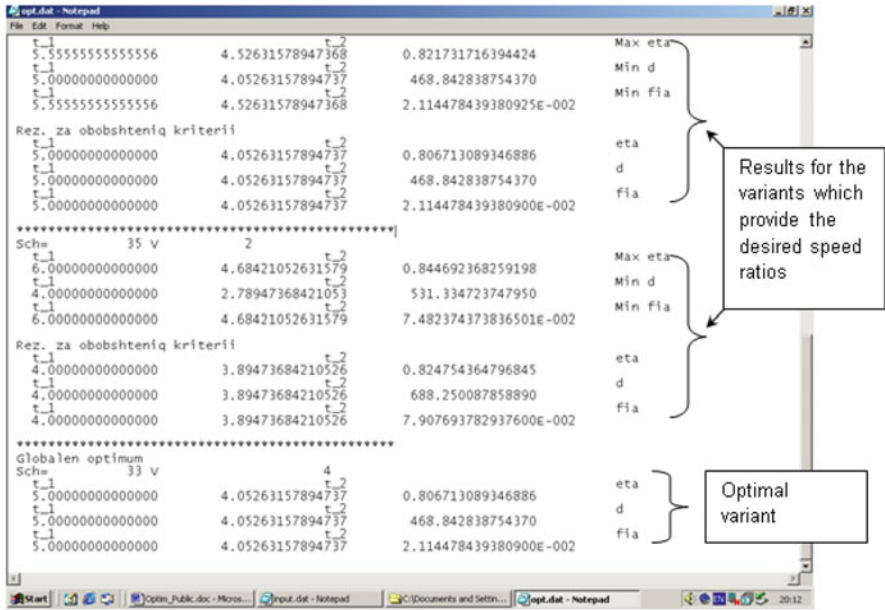
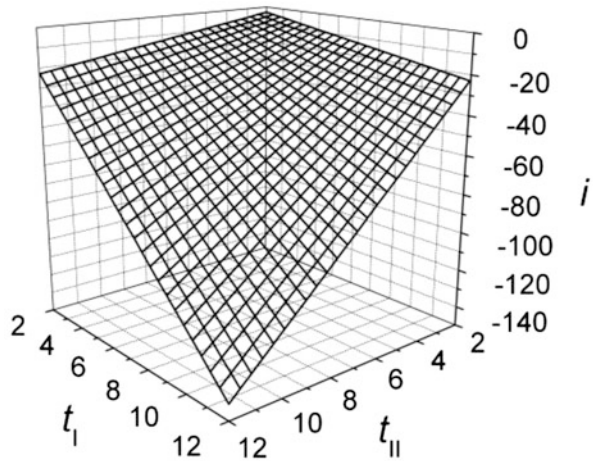


Fig. 8.13 Result of the optimization of all variants providing the desired speed ratios

Fig. 8.14 Total speed ratio as a function of torque ratios t_I and t_{II} of scheme S13WN (E)



8.3 Program 2-BRZ

Developed 2-BRZ program (software) is intended for investigation of single-speed and two-speed two-carrier PGTs. It is written in the Compaq Visual Fortran Professional Edition 6.6.0. The program has three subprograms for:

- Analysis of characteristics of arbitrary variant.
- Synthesis of all solutions that meet the set requirements.
- Evaluation of the solution.

A description of its subprogram (modules) is given below.

8.3.1 Subprogram for PGT Characteristics Analysis

This subprogram enables the generation of sets of different characteristics of each of the PGT variants according to the given input data in the *input* file and recording these sets in a file. This allows engineering visualization of large data sets and comprehensive analysis. In order to speed up the response of the program, there is also the possibility to obtain a reduced record of the data sets of the analyzed variant of the PGT.

Reduced record contains data on the PGT variant at given intervals of torque ratios t_I and t_{II} . These data are:

- Achievable gear ratios.
- Teeth numbers of planets.
- Planets modules.

Reference diameters of ring gears

- Ratios of reference diameters of ring gears.
- Approximate masses of gears (sun gear, ring gear, and planets) in component PGT.
- Approximate mass of gears in compound PGT.
- Calculated efficiency of compound PGT.
- Dispersion of the calculated efficiency shown by standard deviation.
- Relative speeds of planets.
- Forces on planet bearings.
- Torques on the brake shafts.

The complete set, in addition to the above data, also contains:

- Rotational speeds of all elements.
- Torques on all elements.
- Power on all elements.
- Relative (rolling) power in both component PGTs.

All the above data is accompanied by an ordered pair of torque ratios t_I and t_{II} of component PGTs so that they can be graphically represented as functions of these ratios. The program also allows the display of the interdependence of the values of

these characteristics, where one or two characteristics can form a domain and the third a codomain.

All output data of the analysis subprogram are entered in the folder *all results* of the developed program *2-BRZ*.

8.3.2 *Subprogram for PGT Variants Synthesis*

The synthesis subprogram returns as a result of all solutions (PGT variants) that meet the requirements from the *input* file of the *2-BRZ* program as well as the sets of their quantitative characteristics. The output data is written to the *results* folder and they are:

- Alphanumeric designation of the compound PGT variant.
- Corresponding torque ratios of component PGTs.
- Corresponding speed ratios.
- Numbers of teeth of ring gears of component PGTs.
- Modules of PGTs meshing.
- Ratios of reference diameters of PGTs ring gears.
- Approximate masses of gears (sun gear, ring gear, and planets) in component PGT.
- Approximate mass of gears in compound PGT.
- Relative speeds of planets.
- Dispersion characteristic of the calculated equivalent² efficiency (standard deviation).
- Possible specific circulated power.

8.3.3 *Subprogram for Evaluation of the Solution*

The solution evaluation subprogram enables the ranking of the compound PGT variants according to the criteria covered by the complex global objective function and the selection of optimal solution.

The minimum of the global objective function $Z_{gl\ min}$ gives, conditionally speaking, the optimal solution. Namely, this solution is a recommendation of a program in which the most important criteria are expressed by weight coefficients. Due to the impossibility of the mathematical model to cover all criteria that affect the quality of the solution, as well as the problem of lack of information for exact values of the weight of the criteria, it is strongly recommended to critically evaluate solutions from the aspect of criteria not covered by the mathematical model.

²*Equivalent efficiency* is calculated for two-speed PGTs on the base of efficiencies in work with both speeds (i_1 and i_2) considering relative working time of each of them.

In the output file *rank* in the *results* folder (program *2-BRZ*) with the ordinal number indicating the position of each variant of the compound PGT on the priority scale, the program system returns:

- Compound PGT variant designations with corresponding weight coefficients.
- The value of the global objective function, i.e., the quantitative evaluation of the solution.
- The corresponding torque ratios t_I and t_{II} of component PGTs.
- Achievable speed ratio of compound PGT (total speed ratio).
- Dispersion of equivalent efficiency determined by standard deviation.
- Reference Diameter of the Larger Ring Gear (Indicator for Overall Dimension of Compound PGT)
- Ratio of the reference diameters of the ring gears of larger and smaller component PGT.
- Approximate mass of gears in compound PGT.
- Rotational speed of the fastest planet.
- Modules of PGTs meshing.
- The minimum required dynamic load capacity of the most loaded planet bearing.

8.3.4 *Input Data*

So far, the possibilities of the program in the form of output are listed. In order to obtain the output data, input data must be entered. The input data is entered in the *input* file (program *2-BRZ*). Some of them will be shown in the following examples.

8.4 Examples of Selection of the Optimal Compound PGT Variant

8.4.1 *Optimal Choice of Single-Speed PGT*

In case the goal is to arrange a single-speed PGT (Table 8.1), the program will generate a set of variants of single-speed PGTs that can meet the set requirements. Each variant of this set, in the general case, has a set of ordered pairs of torque ratios t_I and t_{II} , where each individual ordered pair enables the realization of the required total speed ratio in its tolerance interval. All arranged pairs within the corresponding variant enable the realization of the required speed ratio, but with different overall dimensions of component PGTs, different efficiency, different relative speeds of planets, etc. The program can find the most acceptable ordered pair of torque ratios

guided by selected criteria. The criteria are accompanied by certain weight coefficients which describe their importance—see formula (8.77).

With a given torque on the input shaft of $T_A = 50 \text{ Nm}$, the required total speed ratio $i = 30.5 \pm 0.5$, and the number of teeth of sun gears $z_{1I} = z_{1II} = 18$, the program provides solutions. Secondary input data is not shown in this example.

The program makes it possible to compare all variants of the compound PGT with each other and to obtain a priority list of variants with their optimal parameters according to the weights of the selected criteria.

For three different combinations of weights, the program generates three files with a list of PGT variants by priority that can achieve the given total speed ratio. In Table 8.12, Table 8.13, and Table 8.14, variant designations with some basic data are listed.

From Table 8.12 it can be seen that according to this criterion the optimal variant is 66NE(W). This variant has the smallest radial dimensions $d_{3\text{max}} = 180 \text{ mm}$, but it has a relatively low degree of efficiency $\eta = 0.481$. The second variant is 26WE(N) with an ordered pair of torque ratios (6, 3.3333) which has a slightly larger dimension $d_{3\text{max}} = 195 \text{ mm}$ and a significantly higher efficiency $\eta = 0.964$.

The analysis of Table 8.13 shows that according to the criterion of the highest efficiency, the optimal variant is 26WE(N) with an ordered pair of torque ratios (4.1667, 5) and the calculated efficiency $\eta = 0.966$. The priority list shows that the

Table 8.12 Priority list of PGT variants with associated parameters obtained with weight coefficients $\chi_a = 1$, $\chi_n = 0$

Variants	Z_{gl}	t_I	t_{II}	i	η	$d_{3\text{max}}$, mm	$d_{3\text{max}}/d_{3\text{min}}$
S66NE(W)	0	3.8333	4	30	0.481	180	1.043
S26WE(N)	0,02717	6	3.3333	30.333	0.964	195	1.032
S55NE(W)	0,03261	3.6667	3.1667	30.555	0.734	198	1.069
S26WN(E)	0,04484	6	3.5	-30.5	0.964	204.75	1.083
S16WN(E)	0,04484	6.5	3.5	30.25	0.964	204.75	1
S33NE(W)	0,05299	5	5.1667	31	0.462	209.25	1.033
S16WE(N)	0,05435	6.6667	3.5	-30	0.963	210	1.025
S44NE(W)	0,0625	3.1667	3.6667	30.555	0.734	214.5	1.075
S23WN(E)	0,08016	6.6667	3.8333	30.389	0.963	224.25	1.068
S23WE(N)	0,08967	8.5	3.1667	-30.083	0.958	229.5	1.074
S13WN(E)	0,09239	8.5	3.6667	-30.167	0.959	231	1.007
S13WE(N)	0,09239	8.3333	3.6667	30.555	0.960	231	1.027
S44NE(W)	0,12228	5	4.1667	-30	0.806	247.5	1.1
S55NE(W)	0,12228	4.1667	5	-30	0.806	247.5	1.1
S22NE(W)	0,22826	4	4.1667	-30	0.461	306	1.02
S33NE(W)	0,2731	10.5	10.1667	-30.5	0.521	330.75	1.033
S66NE(W)	0,29348	9.5	9.1667	-30.5	0.538	342	1.036
S11NE(W)	0,30435	5	4.8333	30	0.465	348	1.031
S11NE(W)	0,32609	5	5.1667	-30	0.444	360	1.032
S22NE(W)	0,86957	9.1667	8.8333	30.5	0.558	660	1.038

Table 8.13 Priority list of PGT variants with associated parameters obtained with weight coefficients $\chi_d = 0, \chi_n = 1$

Variant	Z_{gl}	t_I	t_{II}	i	η	d_{3max}, mm	d_{3max}/d_{3min}
S26WE(N)	0	4.1667	5	31	0.966	247.5	1.886
S16WN(E)	0.00098	5	5	31	0.965	247.5	1.571
S23WN(E)	0.00098	5	5	31	0.965	270	1.714
S26WN(E)	0.00137	4.3333	5	-31	0.965	270	1.978
S23WE(N)	0.00246	5	5.1667	-31	0.964	279	1.771
S16WE(N)	0.00246	5.1667	5	-31	0.964	247.5	1.520
S13WE(N)	0.00496	5.1667	6	31	0.963	297	1.825
S13WN(E)	0.00653	5.3333	6	-31	0.962	297	1.768
S55NE(W)	0.07694	12	8.3333	30.54	0.926	432	1.28
S44NE(W)	0.07694	8.3333	12	30.54	0.926	432	1.28
S55NE(W)	0.08717	8.3333	11.8333	-30.55	0.920	426	1.262
S44NE(W)	0.08717	11.8333	8.3333	-30.55	0.920	426	1.136
S66NE(W)	0.77995	8.8333	9.1667	30.5	0.559	330	1.038
S22NE(W)	0.77995	9.1667	8.8333	30.5	0.559	660	1.038
S11NE(W)	0.80696	10	9.6667	30	0.545	696	1.031
S33NE(W)	0.81254	9.8333	10.1667	30.5	0.542	320.25	1.034
S22NE(W)	0.81955	9.1667	9.5	-305	0.538	684	1.036
S66NE(W)	0.81955	9.5	9.1667	-305	0.538	342	1.036
S11NE(W)	0.84752	10	10.3333	-30	0.524	720	1.032
S33NE(W)	0.85269	10.5	10.1667	-30.5	0.521	330.75	1.033

Table 8.14 Priority list of PGT variants with associated parameters obtained with weight coefficients $\chi_d = 0.5, \chi_n = 0.5$

Variant	Z_{gl}	t_I	t_{II}	i	η	d_{3max}, mm	d_{3max}/d_{3min}
S26WE(N)	0.01503	6	3.3333	30.333	0.964	195	1.031
S16WN(E)	0.02377	6.5	3.5	30.25	0.964	204.75	1
S26WN(E)	0.02431	6	3.5	-30.5	0.964	204.75	1.083
S16WE(N)	0.0295	6.6667	3.5	-30	0.963	210	1.026
S23WN(E)	0.04272	6.6667	3.8333	30.389	0.963	224.25	1.068
S23WE(N)	0.05048	7.3333	3.6667	-30.555	0.961	231	1
S13WE(N)	0.05153	8.3333	3.6667	30.555	0.960	231	1.027
S13WN(E)	0.05269	8.5	3.6667	-30.167	0.959	231	1.006
S55NE(W)	0.18314	7	5.5	30.333	0.872	283.5	1.041
S55NE(W)	0.19463	5.6667	7.1667	-30.852	0.866	290.25	1.035
S44NE(W)	0.20058	5.1667	6.5	30.063	0.863	292.5	1.144
S44NE(W)	0.21317	6.6667	5.3333	-30.666	0.857	300	1.136
S66NE(W)	0.46493	3.8333	4	30	0.481	180	1.043
S33NE(W)	0.50931	5	5.1667	31	0.462	209.25	1.033
S66NE(W)	0.55651	9.5	9.1667	-30.5	0.538	342	1.036
S33NE(W)	0.56289	10.5	10.1667	-30.5	0.521	330.75	1.033
S22NE(W)	0.59804	4	4.1667	-30	0.461	306	1.020
S11NE(W)	0.63184	5	4.8333	30	0.465	348	1.031
S11NE(W)	0.66304	5	5.1667	-30	0.444	360	1.032
S22NE(W)	0.82476	9.1667	8.8333	30.5	0.559	660	1.038

first eight mentioned variants of PGT have the same value of efficiency, so when choosing the best variant, the variant that is better according to other criteria can be chosen.

The analysis of Table 8.14 shows that taking into account both criteria with equal weights, the best choice is the variant 26WE(N) with an ordered pair of torque ratios (6, 3.3333) which has a reference diameter of radially larger ring gear $d_{3\max}=195$ mm and calculated efficiency $\eta=0.964$. In this variant, the degree of efficiency does not change significantly with all three combinations of weight coefficients.

In the same way, an optimal solution for different input data can be sought. The program will offer a list of solutions based on the criteria with which it works, and based on the list of solutions, the designer can choose the appropriate variant of the PGT, guided by criteria that are not built into the logic of the program.

8.4.2 Optimal Choice of Two-Speed PGT

Compound PGTs with two internal and four external shafts (Table 8.2) are investigated. For operating with $F=1$ degree of freedom, the brake on one of the external shafts is needed. These PGTs are appropriate to realize two speed ratios (i_{Br1} and i_{Br2}) with two brakes (Br1 and Br2) on two external shafts. Three locations of both brakes are possible [27, 49]:

- Brakes on both compound shafts (Fig. 8.15a).
- Brakes on both single shafts (Fig. 8.15b).
- Brakes on a single and on a compound shaft (Fig. 8.15c).

All possible working modes (brakes' location and power flow direction) of all variants are checked through the optimization procedure. The variants are described by number from Table 8.2 and indication of input and output shafts (by letters according to the four directions of the world—W-west, N-north, E-east, and S-south). For example, S16NW means Scheme 16 from Table 8.2 with top (N-north) shaft as input and left (W-west) shaft as output.

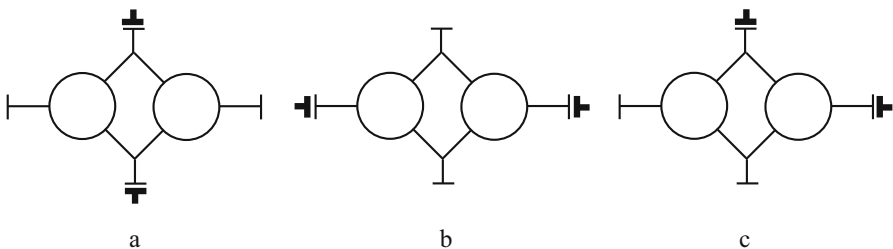


Fig. 8.15 Possible locations of both brakes at two-carrier PGT with four external shafts: a) Brakes on both compound shafts. b) Brakes on both single shafts. c) Brakes on a single and on a compound shaft

Two of more common cases of these PGT applications are investigated below.

Example A: Two-speed compound PGT with positive speed ratios

To show how the program can help set up a two-speed PGT, the following example is shown. Some relevant inputs are:

- Number of required speed ratios is 2: $9.8 \leq i_1 \leq 10$ and $3.9 \leq i_2 \leq 4$.
- Intervals of torque ratios are $2 \leq t_{I} \leq 12$ and $2 \leq t_{II} \leq 12$.
- Numbers of teeth of sun gears are $z_{1I} = 18$ and $z_{1II} = 18$.
- Relative working times with every speed ratio (i_1 and i_2) are $\alpha_{i1} = 0.7$ (70%) and $\alpha_{i2} = 0.3$ (30%).
- Input torque is $T_A = 50$ Nm and input speed is $n_A = 2850 \text{ min}^{-1}$.

Based on the 2-BRZ program, results are obtained that show the basic parameters of PGT variants that can realize the required speed ratios. Some of the basic parameters of these variants are listed in Table 8.15, Table 8.16, and Table 8.17.

Table 8.15 Priority list of solutions obtained with weighting coefficients $\chi_d = 1, \chi_n = 0$

Priority	Scheme	t_I	t_{II}	i_1	i_2	$d_{3 \text{ max}}, \text{ mm}$	η_{eq}
1.	S16WN	3	2	10	4	117	0.953
2.	S55NE	5	3	10	4	157.5	0.930
3.	S13WE	5	2	10	4	157.5	0.940
4.	S36SE	4.833	8.833	9.833	3.912	238.5	0.986
5.	S33SN	3	8.833	9.833	4	238.5	0.984
6.	S12WN	8.833	2	9.833	3.944	238.5	0.979

Table 8.16 Priority list of solutions obtained with weighting coefficients $\chi_d = 0, \chi_n = 1$

Priority	Scheme	t_I	t_{II}	i_1	i_2	$d_{3 \text{ max}}, \text{ mm}$	η_{eq}
1.	S36SE	4.833	8.833	9.833	3.912	238.5	0.986
2.	S33SN	3	8.833	9.833	4	238.5	0.984
3.	S12WN	8.833	2	9.833	3.944	238.5	0.979
4.	S16WN	3	2	10	4	117	0.953
5.	S13WE	5	2	10	4	157.5	0.940
6.	S55NE	5	3	10	4	157.5	0.930

Table 8.17 Priority list of solutions obtained with weighting coefficients $\chi_d = 0.5, \chi_n = 0.5$

Priority	Scheme	t_I	t_{II}	i_1	i_2	$d_{3 \text{ max}}, \text{ mm}$	η_{eq}
1.	S16WN	3	2	10	4	117	0.953
2.	S36SE	4.833	8.833	9.833	3.912	238.5	0.986
3.	S33SN	3	8.833	9.833	4	238.5	0.984
4.	S12WN	8.833	2	9.833	3.944	238.5	0.979
5.	S13WE	5	2	10	4	157.5	0.940
6.	S55NE	5	3	10	4	157.5	0.930

The analysis of Table 8.15, which was obtained only according to the criterion of minimum dimensions ($\chi_d = 1$), shows that the smallest radial dimensions of the larger ring gear are obtained with the S16WN variant with an ordered pair of torque ratios t_I and t_{II} (3; 2). In this case, the reference diameter of the larger ring gear is $d_{3\max} = 117$ mm. It can be seen that in this variant the mass is also the smallest. The calculated equivalent efficiency is $\eta_{eq} = 0.953$.

The analysis of Table 8.16, obtained only according to the criterion of the maximum equivalent efficiency ($\chi_\eta = 1$), shows that S36SE is the variant with the highest efficiency. The calculated efficiency is $\eta_{eq} = 0.986$, but the reference diameter of the larger ring gear is $d_{3\max} = 234$ mm—significantly larger than the reference diameter of the best variant from Table 8.15 (117 mm).

The analysis of Table 8.17 obtained according to both criteria with the same weighting coefficients ($\chi_d = 0.5$ and $\chi_\eta = 0.5$) shows that the optimal variant is S16WN, as in the case of $\chi_d = 1$ and $\chi_\eta = 0$.

It is observed that changing the weight of the criteria changes the value of the global function of the target, and thus the position of the variants in the priority list.

With two-speed PGTs, only one combination of torque ratios t_I and t_{II} can give the required speed ratios. This means that when choosing the optimal solution, they cannot vary in the search for torque ratios because otherwise the speed ratios would also change. Numerous computer syntheses of various solutions show that two-speed two-carrier PGT do not have a large number of variants that can meet the kinematic requirements. This makes it relatively easier to choose the right solution.

Example B: Reversible two-speed compound PGT

Reversible two-speed compound PGTs can provide different speeds (by absolute value) in every direction (appropriate for technological machines with slow working and fast retrieval movement) or equal speeds in both directions—mainly used in vessels [27, 47, 49–51, 70]. The second case is investigated below.

Some relevant inputs are:

- Number of required speed ratios is 2: $-4.6 \leq i_1 \leq -4.4$ and $4.4 \leq i_2 \leq 4.6$.
- Intervals of torque ratios of component PGTs are $1.4 \leq t_I \leq 6$ and $1.4 \leq t_{II} \leq 6$.
- Relative working times with every speed ratio are $\alpha_{i1} = 0.9$ (90%) and $\alpha_{i2} = 0.1$ (10%).
- Input torque is $T_A = 3000$ Nm and input speed is $n_A = 1800$ min⁻¹.

It is necessary to determine the torque ratios t_I and t_{II} , actual speed ratios i_1 and i_2 , teeth numbers of all gears, and efficiency. All component PGTs are with $k = 3$ planets.

Based on the 2-BRZ program, results are obtained that show the basic parameters of PGT variants that can realize the required gear ratios. Some of the basic parameters of these variants are listed in Table 8.18, Table 8.19, and Table 8.20. The speed ratios are indicated as i_{Br1} and i_{Br2} in dependence on the locked brake—Br1 or Br2 (Table 8.20). Marked (colored) values of efficiency are for forward speed of the boat (at which it mainly operates).

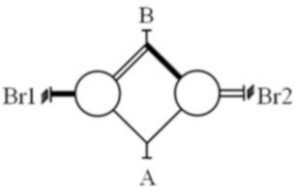
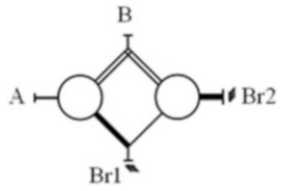
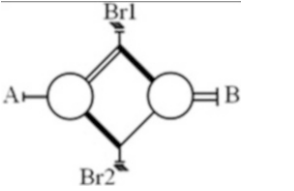
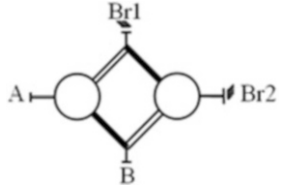
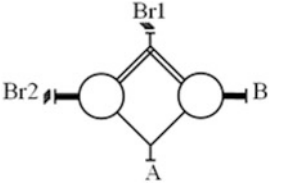
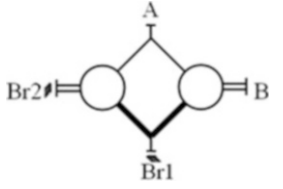
Table 8.18 Main parameters of both component PGTs

Scheme	t_I	t_{II}	z_{1I}	z_{2I}	z_{3I}	z_{1II}	z_{2II}	z_{3II}
S36SN	3.5	4.55	14	17	49	20	35	91
S16WE	1.714	1.604	42	15	72	53	16	85
S33SE	1.714	4.437	42	15	72	16	27	71
S13WN	3.5	1.553	14	17	49	47	13	73
S12WS	4.55	1.553	20	35	91	47	13	73
S55NE	1.714	3.4	42	15	72	15	18	51

Table 8.19 Speed ratios and efficiencies of compound PGTs

Scheme	i_{Br1}	i_{Br2}	η_{oI}	η_{oII}	η_{Br1}	η_{Br2}
S36SN	4.5	-4.55	0.973	0.985	0.979	0.985
S16WE	-4.464	4.407	0.976	0.978	0.962	0.976
S33SE	-4.438	4.422	0.976	0.980	0.980	0.959
S13WN	4.5	-4.436	0.973	0.973	0.979	0.934
S12WS	-4.55	4.573	0.985	0.973	0.985	0.969
S55NE	4.4	-4.475	0.976	0.974	0.980	0.924

Table 8.20 Acceptable solutions (A-input shaft; B-output shaft)

No.	Scheme	Structural scheme	No.	Mark	Structural scheme
1	S36SN		4	S13WN	
2	S16WE		5	S12WS	
3	S33SE		6	S55NE	

8.5 Concluding Remarks

This chapter discusses a method for optimal selection of a structural scheme and its parameters of compound two-carrier PGTs. The optimization methodology is based on the torque method, which makes it easy and understandable for the engineer. The optimization procedure is demonstrated on compound two-carrier planetary gear trains with three external shafts. Due to the limited volume of this chapter, the authors have not shown the peculiarities of the application of the method in other more complex two- and multi-carrier PGTs, but the main things are the same.

According to the presented methodology, an optimization procedure for selection of structural scheme and its parameters for two-speed change-gears on the base of compound two-carrier PGTs with four external shafts has been developed, details of which can be found in [42, 47, 49, 50]. Other aspects of these interesting PGTs can be found in [48, 70–72].

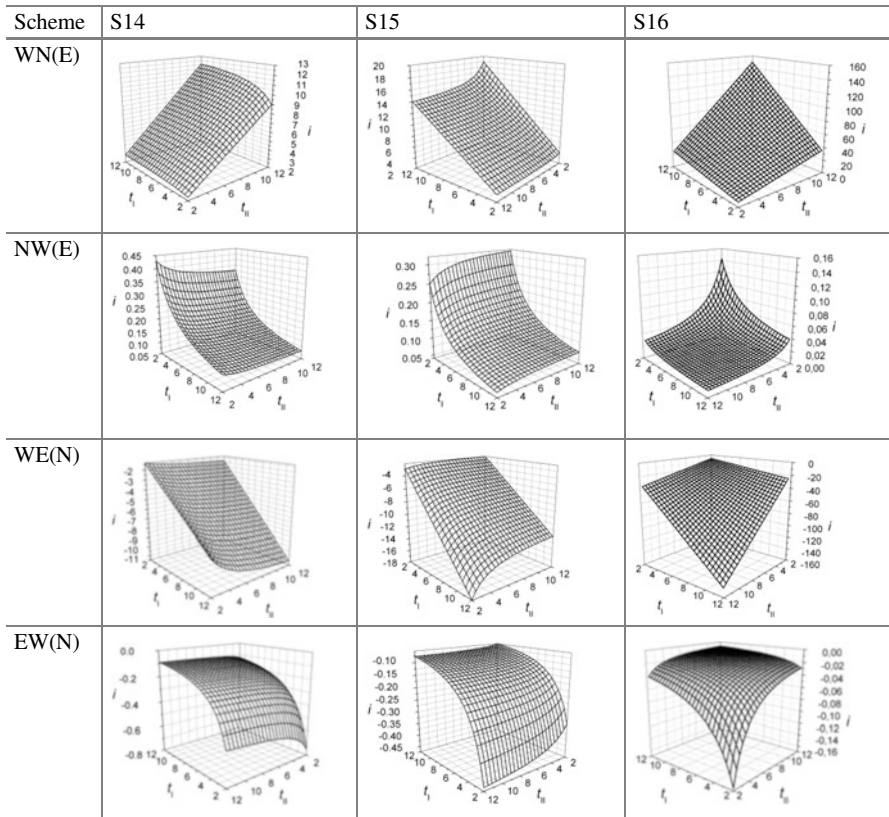
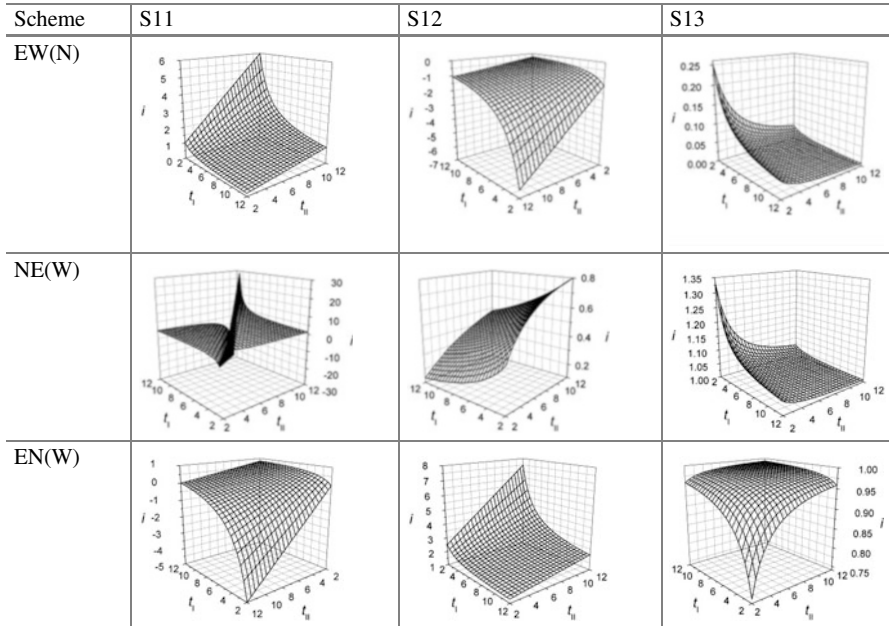
The proposed methodology is also suitable for more complex multi-carrier PGTs.

Appendix 8.1

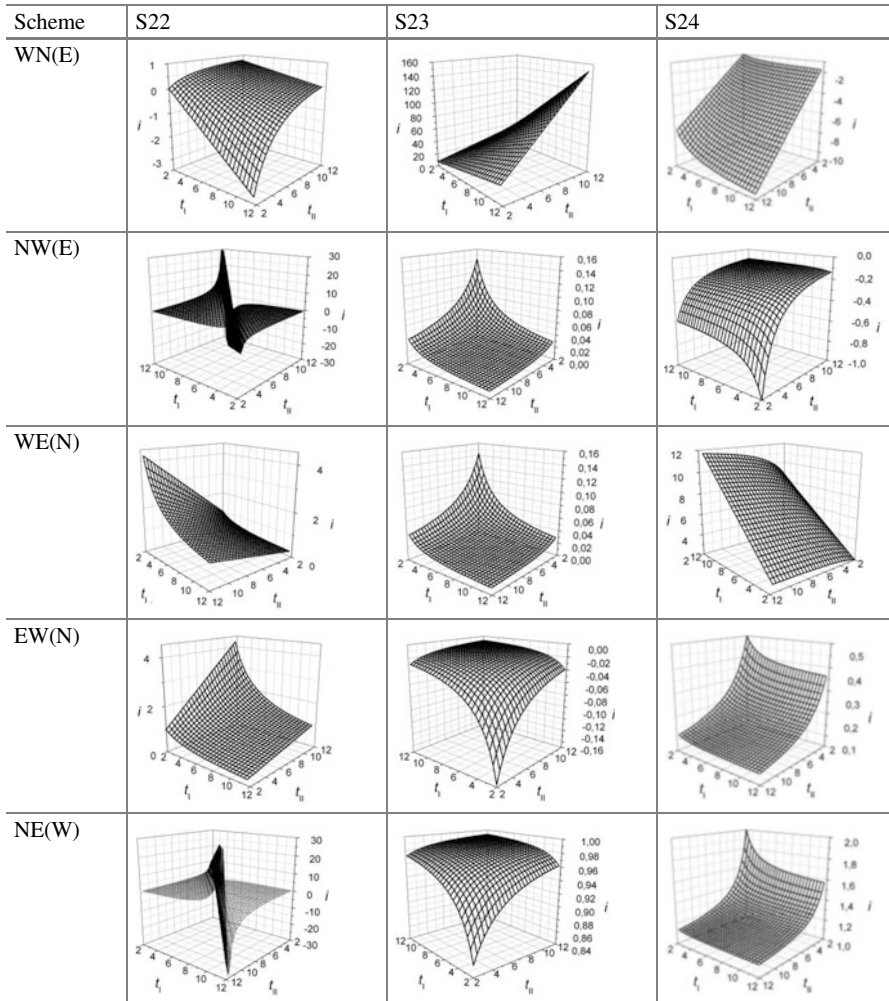
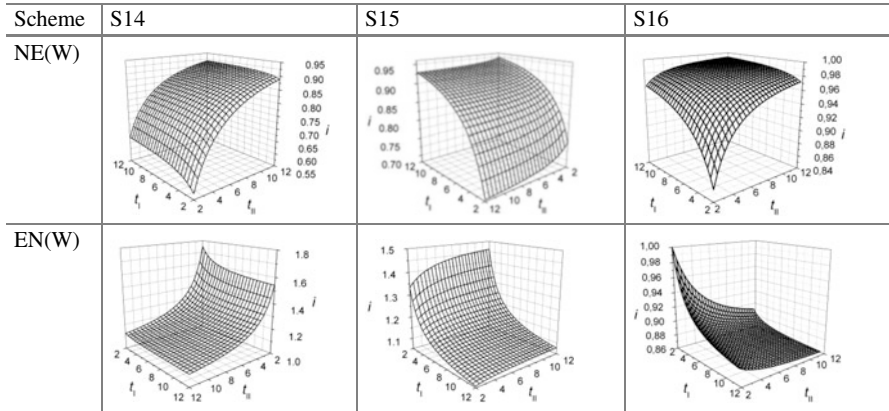
Total speed ratio i of six working modes of compound PGTs from Table 8.1 as a function of torques ratios t_I and t_{II} of component PGTs.

Scheme	S11	S12	S13
WN(E)			
NW(E)			
WE(N)			

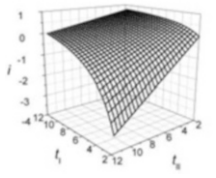
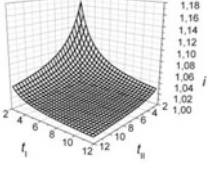
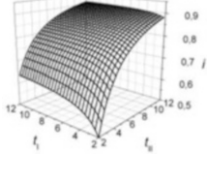
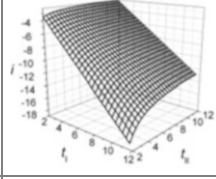
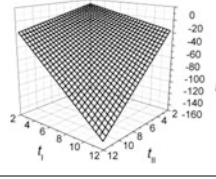
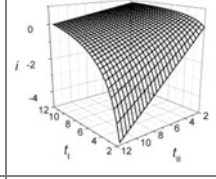
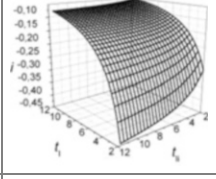
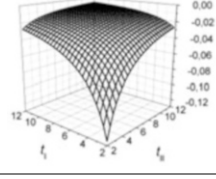
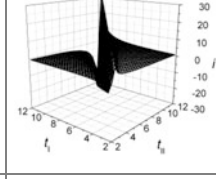
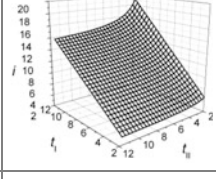
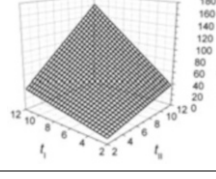
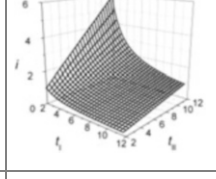
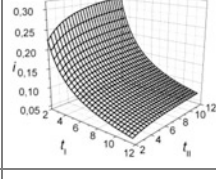
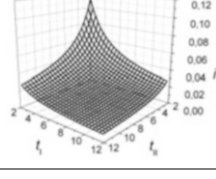
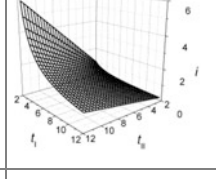
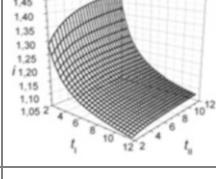
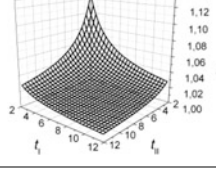
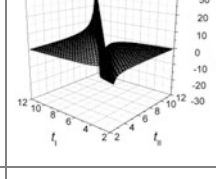
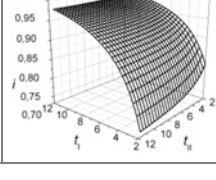
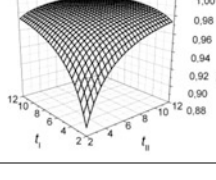
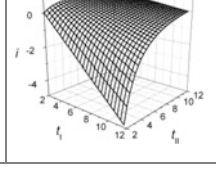
(continued)

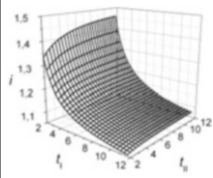
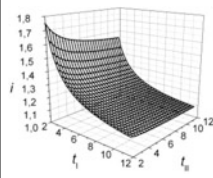
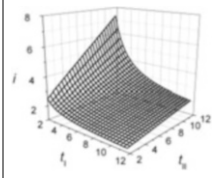
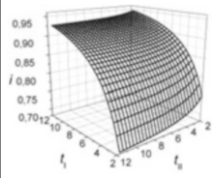
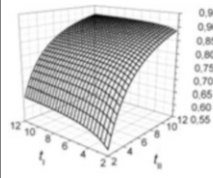
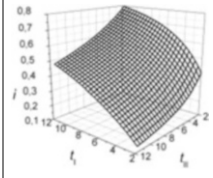
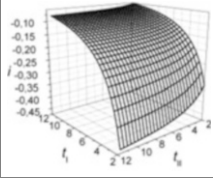
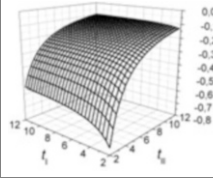
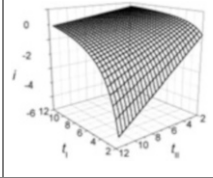
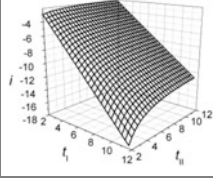
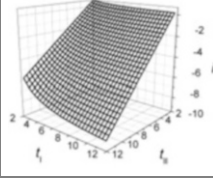
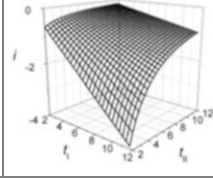
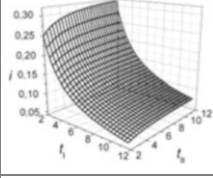
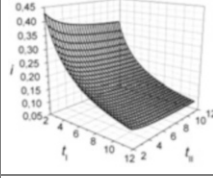
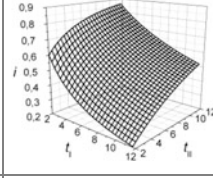
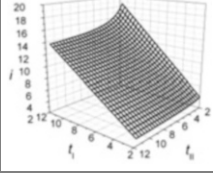
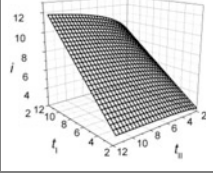
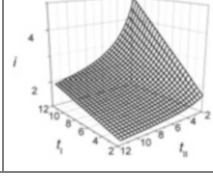


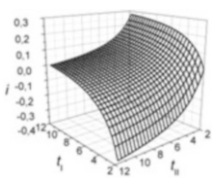
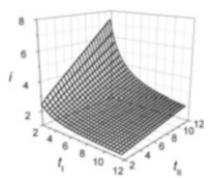
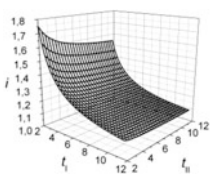
(continued)



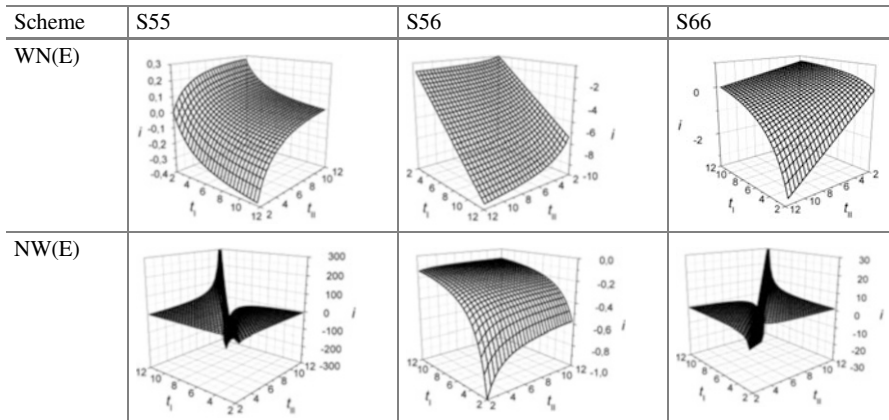
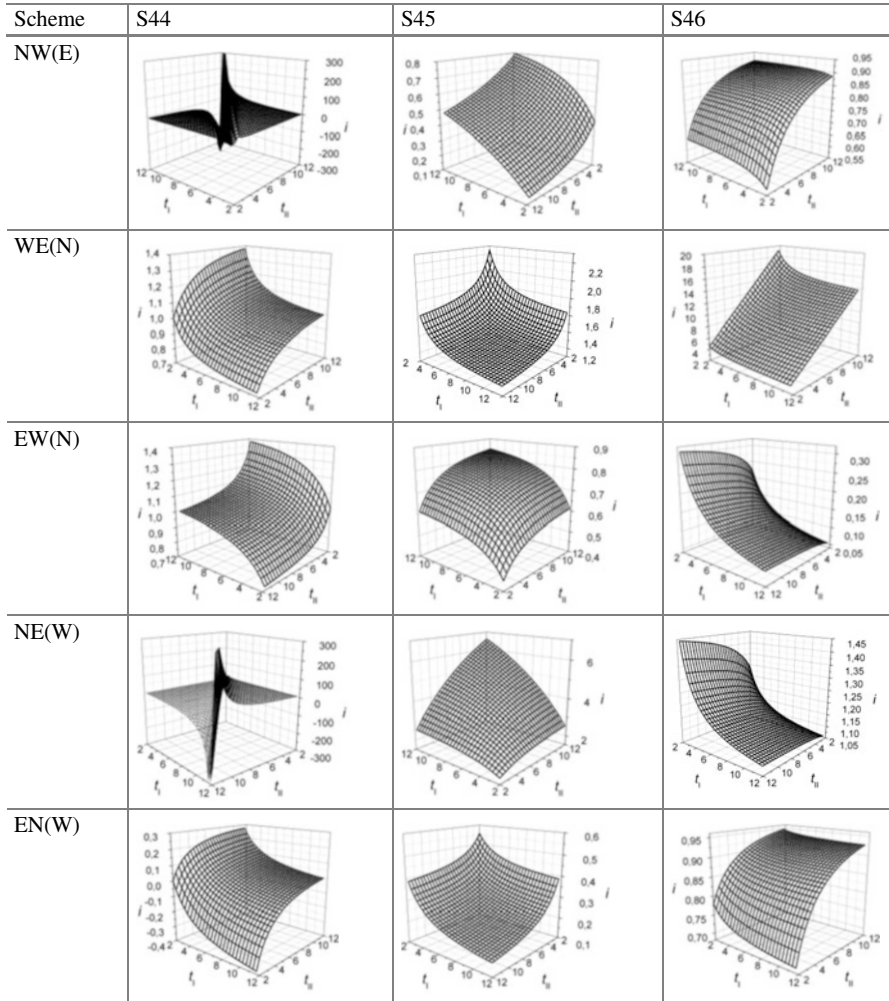
(continued)

Scheme	S22	S23	S24
EN(W)			
WN(E)			
NW(E)			
WE(N)			
EW(N)			
NE(W)			
EN(W)			

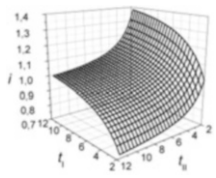
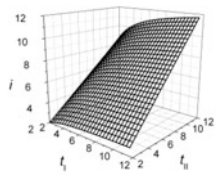
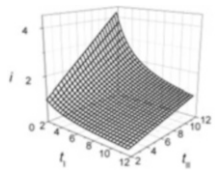
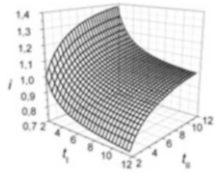
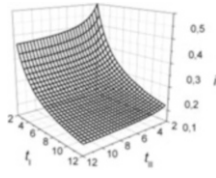
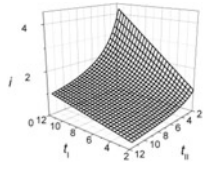
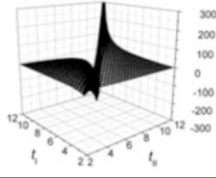
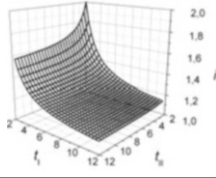
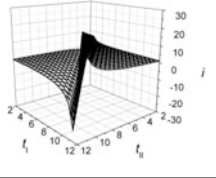
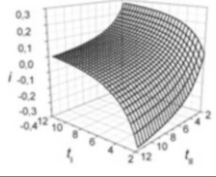
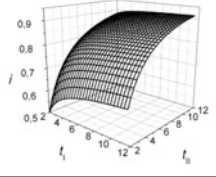
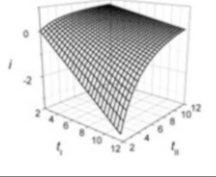
Scheme	S34	S35	S36
WN(E)			
NW(E)			
WE(N)			
EW(N)			
NE(W)			
EN(W)			

Scheme	S44	S45	S46
WN(E)			

(continued)



(continued)

Scheme	S55	S56	S66
WE(N)			
EW(N)			
NE(W)			
EN(W)			

References

1. Dimchev, G. (2000). *Geometrical and technical-economical optimization of gear trains. Habilitation Thesis.* Sofia: Technical University. (in Bulgarian).
2. Goll, S. (1980). Einfluss auf die Tragfähigkeit Zahnrad. *Maschinenbautechnik*, 86.
3. Linke, H. And G. Gayewski. Breitenlastverteilung unter besonderen Berücksichtigung bei Verzahnungen. *Maschinenbautechnik*. 1983, Nr.10.
4. Roth, K., Kollenroth, F. Zahnradpaarungen mit komplementprofilen. *Konstruktion*. 1982, Nr. 3.
5. Shaker, M., T. Zou, J. Angeles, and A. Morozov. Optimization of tooth-root profile for maximum load-carrying capacity: spur and bevel gears. *CCToMM Mechanisms, Machines, and Mechatronics (M³) Symposium, Ottawa, Ontario: May 28 and 29, 2015.* http://iftomm.net/images/Documents/ConferenceProceedings/CCToMM_2015.pdf
6. Satoshi, Oda. Study on bending fatigue strength of gears. // Bull. ISME, Nr.177, 1980.
7. Zhuravlev, G.A. and G.A. Ageev. Synthesis of spur gear trains with minimal bending stresses. *Vestnik Mashinostroenia* 1982, No 2. (in Russian).
8. Stoyanov, S., A. Dobrova, and V. Dobrev. Design system for gear trains in the environment of SolidWorks®. *Proceedings of the "Power Transmissions 2006", Novi Sad, Serbia, 25–25 April 2006*, pp. 91–94.
9. Gushchin, V. G., & Ostrovskiy, G. N. (1980). Spur gear train with multidirectional deviations of the pitch of gearing. *Izvestiya VUZ Mashinostroenie, 11.* (in Russian).

10. Leistner, F. And E. Freitag. Einfluss deer Taumelabweichung auf das Tragbild bei Stirnradgetrieben. *Maschinenbautechnik*. 1979, Nr.10.
11. Teraushi, Y., H. Nadano, and N. Miaoru. On the effect of the tooth profile modification on the dynamic load of the spur gear. *Bull. ISME*, Nr. 207, 1982.
12. Ma, H., Pang, X., Feng, R., & Wen, B. (2016). Evaluation of optimum profile modification curves of profile shifted spur gears based on vibration responses. *Mechanical Systems and Signal Processing*, 70-71, 1131–1149. <https://doi.org/10.1016/j.ymssp.2015.09.019>.
13. Vulić, A. And J. Stefanović-Marinović. Design parameters for planetary gear transmissions optimization. *Proceedings of the "Power Transmissions 2006"*, Novi Sad, Serbia, 25–25 April 2006, pp. 137–142.
14. Klein, B., and Z. Li. Analytisches Verfahren zur parametrischen Optimierung von Zahnradgetrieben. *Antriebstechnik*. 1995, Nr. 3, S. 75–78.
15. Lambin, L. N. (1983). Assignment of displacement factors in the automated design of gear trains. *Vestnik Mashinostroeniya*, 6. (in Russian).
16. Karaivanov, D. (2009). X-Gear – an European project in help of gear trains manufacturers. *Machines Technologies Materials*, 3(3–4), 3–8. (in Bulgarian).
17. Concli, F., & Coenen, J. (2015). Low-lost gears for precision planetary gearboxes: Influence of the gear design on the meshing and the churning power losses. *VDI-Berichte*, 2255-1, 53–65. ISSN 0083-5560.
18. Concli, F., & Gorla, C. (2013). A new methodology for the prediction of the no-load losses of gears: CFD an experimental investigation of the efficiency of a planetary gearbox. *VDI-Berichte*, 2199-2, 1125–1137. ISSN 0083-5560.
19. Hohn, B. -R., K. Stahl and P. Gwinner. Improved efficiency for high-ratio planetary gear transmission for wind turbines – Low-loss Wolfrom transmission for wind turbines. *VDI-Berichte* 2199–2202, 2013, pp. 1113–1124. ISSN 0083-5560.
20. Kruszynski, B. Einfluss des Walzfraserverschleisses auf die Eigenspannungen von Zahnradern. *Werkstoff und Betrieb*, 1981, Nr. 9.
21. Gulya, Z. N. (1981). *Durability control of cylindrical gear wheels*. Vysshaya Shkola: Lvov. (in Russian).
22. Ponamarev, V. P., & Shchin, D. P. (1981., No. 3). Technological tolerances and dimensions determination in gear cutting process. *Vestnik Mashinostroeniya*. (in Russian).
23. Stefanović-Marinović, J. and M. Milovančević. An application of multicriteria optimization to planetary gear transmissions. *Proceedings of The International Conference Mechanical Engineering in XXI Century*, 25–28 November 2010, Niš, Serbia, pp. 133–136.
24. Norihisa, A., & Susomi, H. (1981). *Research on bending strength properties spur gears without rim*. *Bull. ISME*, Nr195.
25. Tae-Hyong, C., & Toshiyui, S. (1982). Bending stress of internal Spur Gear. *Bull. ISME*, 202.
26. Sholomov, N. M. (1984., No. 4). Stresses determination in the tooth root of thin-rim gears. *Vestnik Mashinostroeniya*. (in Russian).
27. Arnaudov, K., & Karaivanov, D. (2019). *Planetary gear trains* (p. 358). Boca Raton: CRC Press. ISBN 978-1-138-31158-5.
28. Peeken, H. and J. Widanata. Rechnerunterstutze Konstruktioin von Maschinen-gehausen zur Optimierung. *Konstruktion*. 1982, Nr. 6.
29. Pinenkamp, W. Methoden zur Konstruktion und Prufung grosser Zahnradgetrieben. Congr. mond. engrenage, Paris, 1977, Nr. 2.
30. Winter H. Gears & Gear Research. Gearing and transmissions. 1995, No. 1.
31. Ognianović, M. and S. Ćirić-Kostić. Gear disturbance energy transmission through the gear system and frequency spectrum. *Proceedings of the "Power Transmissions 2006"*, Novi Sad, Serbia, 25–25 April 2006, pp. 167–172.
32. Dinev, G. One approach for multicriteria optimization of one stage gear transmission. In *Proceedings of 6th Int. Conference RaDMI 2006, Budva, Montenegro, 13–17 September 2006* (pp. 201–206).

33. Ushakov, M. M. (1985., No. 8). Relative weight of gear trains. *Izvestiya VUZ Mashinostroenie.* (in Russian).
34. Kos, M. Bewertung der Ausgleichssysteme in Planetengetriebe. *Konstruktion*. 1981, Nr. 3.
35. Petrov, Z. V., & Prevalov, V. S. (1984). Minimization of the reduced moment of inertia of two-stage cylindrical gear trains. *Izvestiya VUZ Mashinostroenie*, 12. (in Russian).
36. Week, M., & Gold, P. (1977). *Möglichkeiten und Grenzen bei der Bestimmung des dynamischen Verhaltens von Zahnradgetrieben*. Paris: Congr. mond. engrenage.
37. Arnaudov, K., & Karaivanov, D. (2004). Raum- und Massesparende Zahnradgetriebe. In *Proceedings of the 3rd Conference about Construction, Shaping & Design*. Novi Sad (pp. 73–78).
38. Karaivanov, D. Structural analysis of coupled multi-carrier planetary gear trains – from lever analogy to multi-objective optimization. *Proceedings of the 3rd Int. Conf. on Manufacturing Engineering (ICMEN)*, 1–3 October 2008, Chalkidiki, Greece, pp. 579–588.
39. Rao, S.S. Multiobjective optimization in structural design with stochastic processes. *AIAA Journal*. 1984, 108, No. 4, pp. 1670-1678.
40. Rao, S. S., & Eslampour, H. R. (1986). Multistage multiobjective optimization of gearboxes. *Journal of Mechanisms, Transmissions, and Automation in Design.*, 108, 461–468.
41. Savsani, V., Rao, R., & Vakharia, D. (2010). Optimal weight design of a gear train using particle swarm optimization and simulated annealing algorithms. *Mechanism and Machine Theory*, 45, 531–541.
42. Troha, S., P. Petrov, and D. Karaivanov. Regarding the optimization of coupled two-carrier planetary gears with two coupled and four external shafts. *Machinebuilding and Electrical Engineering*. 2009, **LVIII** (1), pp. 49–55. ISSN 0025-455X.
43. Bozzolo, A., & Zangani, D. (2009). Development of gear drive-trains based on new materials and novel gear systems. In *Proceedings of the 3rd Int. Conf. Power Transmissions '09* (edited by A. Mihailidis), *Kallithea [Greece]* (pp. 249–253). ISBN 978-960-243-662-2.
44. Mihailidis, A. and C. Pupaza. Simulation Driven Design of Internal Gears. Multicriteria optimization of internal gears. *VDI-Berichte*, Nr. 2108, 2010, pp. 725–740.
45. Brüser, P. (1989). Optimierung von Planetengetrieben. *Antriebstechnik*, 28(2), 64–67.
46. Daoudi, K., El-M. Boudi, and M. Abdellah. Genetic Approach for Multiobjective Optimization of Epicyclic Gear Train. *Mathematical Problems in Engineering*. 2019, 9324903, 10, <https://doi.org/10.1155/2019/9324903>.
47. Stefanović-Marinović, J., S. Troha, and M. Milovančević. An application of multicriteria optimization to the two-carrier two-speed planetary gear trains. *Facta Universitatis, Series: Mechanical Engineering*. 2017, **15** (1), pp. 85–95. ISSN 0354–2025 (Print) , ISSN 2335–0164 (Online).
48. Stefanović-Marinović, J., Troha, S., Andelković, B., & Milovančević, M. (2018). Efficiency of planetary gear trains as criterion for optimal solution selection. *Machine Design.*, 3, 95–98. ISSN 1821-1259.
49. Troha, S. (2011). *Analysis of a planetary change gear train's variants*. Dissertation. Croatia: Engineering Faculty, University of Rijeka. (in Croatian).
50. Troha, S., Ž. Vrcan, D. Karaivanov, and M. Isametova. The selection of optimal reversible two-speed planetary gear trains for machine tool gearboxes. *FACTA UNIVERSITATIS, Series: Mechanical Engineering*. 2020, **18** (1), pp. 121–134. ISSN: 0354–2025 (Print), ISSN: 2335–0164 (Online).
51. Troha, S., Stefanović-Marinović, J., Vrcan, Ž., & Milovančević, M. (2020). Selection of the optimal two-speed planetary gear train for fishing boat propulsion. *FME Transactions.*, 48(2), 397–403. ISSN 1451-2092.
52. Tkachenko, B. A. (2003). *Planetary mechanisms*. Kharkov: Kharkov Aviation Institute Publ. (in Russian).
53. Arnaudov, K., & Karaivanov, D. (2001). Engineering analysis of the coupled two-carrier planetary gearing through the lever analogy. In *Proceedings of the International Conference on Mechanical Transmissions* (pp. 44–49). Chongqing, China: China Machine Press.

54. Karaivanov, D. (2000). *Theoretical and experimental studies of influence of the structure of coupled two-carrier planetary gear trains on its basic parameters. Dissertation.* Sofia: University of Chemical Technology and Metallurgy. (in Bulgarian).
55. Karaivanov, D., S. Troha, and R. Pavlova. Experimental study of the losses in a three-stage planetary gear train. *Proceedings of the 3rd Int. Conf. "Power Transmissions '09"*, edited by A. Mihailidis, Kallithea [Greece], 1–2 Oct., 2009, pp. 527–532. ISBN 978-960-243-662-2.
56. Kurth, F. (2012). *Efficiency determination and synthesis of complex-compound planetary gear transmissions. Dissertation.* Munich: Technical University.
57. Niemann, G., & Winter, H. (1995). *Maschinenelemente. Band 2. Zahnradgetriebe – Grundlagen, Stirnradgetriebe. 2. Auflage.* Berlin: Springer-Verlag.
58. Arnaudov, K., & Karaivanov, D. (2017). *Torque method for analysis of compound planetary gear trains* (p. 92). Beau Bassin [Mauritius]: LAP Lambert Academic Publishing. ISBN 978-620-2-01693-3.
59. Arnaudov, K., Alipiev, O., & Karaivanov, D. (2020). Biplanetary gear trains and their analysis through the torque method. In V. Goldfarb, E. Trubachev, & N. Barmina (Eds.), *New approaches to gear design and production* (Mechanisms and Machine Science 81) (pp. 311–322). Springer Nature Switzerland AG. ISSN 2211-0984, ISBN 978-3-030-34944-8, <https://doi.org/10.1007/978-3-030-34945-5>.
60. ISO 6336 Calculation of load capacity of spur and helical gears, 2006.
61. Karaivanov, D. Structural analysis of the coupled planetary gears with considering the efficiency of the coupling gears. *Proceedings of the 2th Int. Conf. on Manufacturing Engineering (ICMEN), Kallithea of Chalkidiki, Greece*, October 5–7, 2005, pp. 381–387. ISBN 960-243-615-8.
62. Predki, W., F. Jarhov F., and J. Kettler. Calculation method for the determination of the oil sump temperature of industrial planetary gears. *VDI-Berichte 1665–1*, pp. 507–522.
63. Karaivanov, D. and S. Troha. On the structural Analysis of Coupled Planetary Gears. *Machinebuilding and electrical engineering*. 2005, Special edition – science edition 9, pp. 76–83.
64. Müller, H. W. (1998). *Die Umlaufgetriebe – Auslegung und vielseitige Anwendungen* (2. Auflage ed.). Berlin: Springer-Verlag.
65. Karaivanov, D., & Popov, R. (2003). Experimental study on the clearances of the two-stage planetary gear. *Journal of the University of Chemical Technology and Metallurgy*, 4(XXXVIII), 1331–1338.
66. Veits, V. L., Kochura, A. E., & Martynenko, A. E. (1971). *Dynamic calculation of machines transmissions* (352 p). Leningrad: Mashinostroenie.
67. Arora, J., & Wang, Q. (2005). Review of formulations for structural and mechanical system optimization. *Structural and Multidisciplinary Optimization*, 30(4), 252–272.
68. Stoyanov, S. (2006). *Optimization of technological systems.* Tehnika: Sofia. (in Bulgarian).
69. Karaivanov, D. Handling machines gearings and their optimal choice. *Zbornik radova sa Naučno-stručnog skupa Istraživanje i razvoj mašinskih elementa i sistema JAHORINA – IRMES'2002, 2/2, Srpsko Sarajevo - Jahorina*, 19. i 20. September 2002, pp. 685–690.
70. Troha, S., D. Karaivanov, and E. Džindo. Two-speed two-carrier planetary gear trains. *7th International Scientific and Expert Conference TEAM 2015, Technique, Education, Agriculture & Management.* Belgrade, Serbia, October 15–16, 2015, pp. 538–542.
71. Troha, S., N. Lovrin, and M. Milovančević. Selection of two-carrier shifting planetary gear train controlled by clutches and brakes. *Transactions of FAMENA*. 2012, XXXVI (3), pp. 1–12. ISSN 1333-1124.
72. Troha, S., Žigulić, R., & Karaivanov, D. (2014). Kinematic operating modes of two-speed two-carrier planetary gear trains with four external shafts. *Transactions of FAMENA*, 38(1), 63–76. ISSN 1333-1124.